Glueball Spectroscopy on a Lattice

David Bosch (s2908808)
University of Groningen
Supervisor: Prof. Elisabetta Pallante

May 29, 2020

Abstract

Lattice quantum chromodynamics (LQCD) has been used to determine the mass of glueball particles since the 1970s. Since then a number of techniques have been developed to reduce the variance of the measured operators. This thesis discusses QCD and LQCD, then shows how the euclidean two-point correlators of the linear combinations of closed Wilson loops on the lattice may be used to determine glueball masses. The algorithms for updating the lattice (psuedo-heatbath), decorrelating configurations (overrelaxation), and reducing variance; multihit, multilevel, variational method are described. Using software in part written by the author the 0^{++} glueball mass is determined on $SU(2)$ using the variance reducing algorithms. The algorithms are compared in terms of accuracy and computational time complexity. This thesis also serves as a validation for the software, so that it may be used for $SU(8)$ glueball mass calculations in the future research to examine the validity of QCD solutions in the large N 't Hooft limit.

Contents

1 Introduction **4**

2 Yang Mills Theory **6**

3 Yang Mills Theory on a Lattice **10**
3.1 Lattice and Discretization 11
3.2 The Wilson Action 13

4 Glueball Operator States **18**
4.1 The Cubic symmetry group 20
4.2 Spin states with respect to the cubic group 23
4.3 Irreducible cubic group representations and corresponding Wilson loops 24

5 Numerical Simulation Details **30**
5.1 Pseudo-Heatbath 35
5.1.1 SU(2) Heatbath 37
5.1.2 The Pseudo-Heatbath for N>2 41
5.2 Overrelaxation 43
5.3 Multihit 45
5.4 Multilevel 46
5.5 Variational Method 48
5.6 Jackknife 49
5.7 Code Architecture 50

6 Results and Discussion **52**
6.1 Setting the scale 52
6.2 Glueball mass estimates 53

7 Conclusion **64**

8 Acknowledgements **66**

A Multiplicity of Irreducible Representations of the Cubic Group in Wilson Loop Operators up to Length 8 **72**

B Spatial Orientations and Constructable Wavefunctions of Additional Operators **74**

C Glueball Correlators and Mass Estimates for $\beta = 1.8$ and 2.2 76

1 Introduction

Quantum chromodynamics (QCD) in its modern form began with the reframing of color as the source of the strong force by Fritzsch, Leutwyler, and Gell-Man[1]. Their principal contribution was to express the strong force as an instance of a Yang-Mills field theory [2], invariant under the special unitary group of order 3. Contrary to previously existing theories such as Quantum Electrodynamics, QCD displayed a number of odd properties most notably what later became known as asymptotic freedom [3, 4]; the interaction strength between particles decreases as the energy scale increases (and correspondingly the length scale decreases). One interesting consequence of this effect is that perturbation theory is only effective for QCD at at UV scales (high energy/short distance), contrary to theories such as QED where it is effective in the IR regime (low energy/high distance).

In response to the difficulties of studying QCD at low energie scales a nonpertubative solution of QCD was found to be lattice QCD (LQCD) [5] (for an overview of early developments see [6]). The theory is placed on a 4-dimensional space-time lattice, with lattice spacing a, with finite volume (given in integer multiples of a). Frequently, such as in this thesis, periodic boundary conditions are also applied. The continuum QCD theory may be described by having lattice spacing $a = 0$ and infinite volume. As such working on the lattice introduces corrections that must be removed through appropriate methods. The lattice itself is a collection of points representing points in space-time separated by a lattice spacing a. Each point is connected to its neighbors by "links", parallel transporters of the gauge field from one point to another. The links are represented by matrices, members of the $SU(N)$ group. In practice these links are stored and updated in simulations. Many developments were formulated on the lattice, including the first evidence of color confinement [5], but also covers such as the strong coupling expansion. The introduction of the lattice did pose problems for the theory as it became discrete. Spherical symmetry was broken and replaced by the much more limited cubic symmetry, resulting in problems of the representation of spin (see chapter 4). Furthermore, at a more basic level the discretization of the derivatives and integrals requires the introduction of a new action, the Wilson action, that recovers the Yang-Mills action in the $a \to 0$ limit (see chapter 3).

Glueballs are massive particles that are predicted by the QCD theory due to the self-interactions of gluons [5]. As pertubative expansions are usually completed around points of the theory in which the interaction strength is near zero, it results in glueballs being difficult to study through such methods.

The lattice offered an effective strategy for the determination of glueball properties, including their masses, glueball to vacuum matrix elements [7, 8], and branching ratios for decays [9]. Knowledge of these properties may be used in experimental conditions to support or oppose particular glueball particle candidates (see for instance [9] or [10]), as well as offer insight into detection ranges for measurement. It may be shown (see chapter 4) that linear combinations of closed loops consisting of links on the lattice are isomorphic to glueball states. By measuring these loops over a large number of lattice configurations, estimates of the glueball mass and other physical properties may be determined.

The lattice represents only a single configuration of the field at any time, and it not representative of the entire theory. As such multiple lattices needed, such that accurate measurements may be produced. This is completed through a Markov Chain Monte Carlo (MCMC) method in which the links of the lattice are updated so that the distribution of lattice configurations accurately reflects the theory. This updating procedure results in correlations between configurations that must accounted for in measurement. A number of updating steps and overrelaxation methods (see chapter 5) are employed to limit these autocorrelations.

In this thesis we focus on measuring the mass of the lowest energy 0^{++} glueball in $SU(2)$. The mass of the glueball may be determined by the correlation of the loops operators described above separated by a time t, along the time axis of the lattice. By varying the time t and of the correlators the glueball mass may be estimate from the logarithm of the correlation function. A number of techniques were used improve the accuracy of the determined masses and to reduce the variance. These methods include the Multihit, Multilevel, and Variational method described in detail in chapter 5. These methods have been compared in terms of accuracy, variance, and computational time required for the gathering of statistics.

The code that was used in the simulations was written by Jelle Bor, Piter Annema and the author. The secondary purpose of this thesis is to test the validity of this code such that it may be used for larger scale simulations. The end goal of which is to determine the glueball masses in $SU(8)$. Marco Bochicchio [11] has proposed a solution for QCD in the large N 't Hooft limit. Simulations of glueballs in at larger N could be used to determine the accuracy of this solution. In previous literature glueball masses have been determine up to $SU(8)$ [12, 13] (see also [14]) however the two independent results contradict one another. The long term hope of this project it to rectify these results and determine an accurate value of glueball masses in $SU(8)$.

The structure of this thesis is as follows. In chapter 2 we briefly describe Yang-Mills theory and how the pure gauge field may be derived from the parallel transport of vectors along a field that is invariant under $SU(N)$. In chapter 3 we translate Yang-Mills theory to the lattice, and describe the Wilson action. In chapter 4 we describe the glueball operator states on the lattice and their relationship to their continuum counterparts. In chapter 5 we describe the numerical simulation, including the updating of the lattice through the pseudo-heatbath and the overrelaxation methods, as well as the measurement and statistical techniques implemented, including Multihit, Multilevel, Variational Method, and the Jackknife estimators. In chapter 6 we describe the numerical results of the simulations. Finally in chapter 7 we summarize and conclude the thesis.

2 Yang Mills Theory

We first discuss Yang Mills theory in the continuum setting, before translating it to a four dimensional lattice. The majority of the fields in the standard model of particle physics are examples of Yang Mills fields, including quantum chromodynamics (QCD). Yang Mills theory concerns itself with Lagrangians consisting of various operators of complex vector fields that are invariant under local group transformations. In this thesis we will focus exclusively on the special unitary group, $SU(N)$.

To discuss this in more detail we examine a complex vector field $\phi(x)$, such that at every point x the vector $\phi(x)$ is an element of a vector space V that is isomorphic to the field $\mathbb{C}^N$. We let the components of $\phi(x)$ be labeled by $\phi^i(x)$ such that i runs from 1 to N. Now we consider a generic Lagrangian:

$$\mathcal{L} = \phi(x) \cdot (\Box + m^2)\phi(x) + U(\phi(x) \cdot \phi(x)) \tag{2.1}$$

in which "$\cdot$" is scalar product on the vector space V defined as $x \cdot y = \sum_i x^{i*} y^i,\ x, y \in V$, $\Box = \partial^\mu \partial_\mu$ the d'Alembert operator, m is a mass and U is a generic potential function of the scalar product of $\phi(x)$ with itself. We note that this Lagrangian is invariant under global $SU(N)$ transformations of the form

$$\phi(x) \to \phi'(x) = \Lambda\phi(x) \quad \Lambda \in SU(N)$$

In fact, all Λ are $N \times N$ unitary matrices with unit determinant, i.e. $\det(\Lambda) = 1$ and $\Lambda^\dagger \Lambda = \mathbf{1}$ where "$\dagger$" is the hermitian conjugate and $\mathbf{1}$ is the $N \times N$ unit matrix.

A larger class of symmetry transformations is that of local, as opposed to global, gauge transformations defined by:

$$\phi(x) \to \phi'(x) = \Lambda(x)\phi(x) \tag{2.2}$$

such that Λ now varies as a function of the spacetime position x. Yang-Mills theory requires that the Lagrangian above be invariant under this local gauge symmetry. As it is not currently, it requires a modification of the Lagrangian with the introduction of a covariant derivative. Covariant derivatives themselves are defined in terms of the transformations of a vector (in the present case ϕ) transported along a curve. As such we first define a curve $\mathscr{L}_{yx}$ to be a directed space-time curve from position x to y. With each possible curve we identify a $SU(N)$ matrix U such that

$$U(\mathscr{L}_{yx}) : V_x \to V_y \tag{2.3}$$

$$\phi(x) \in V_x,\ U(\mathscr{L}_{yx})\phi(x) = \phi'(y) \in V_y \tag{2.4}$$

U is a map from a vector space V_x at position x to a vector space V_y defined at point y. The vector $\phi'(y) = U(\mathscr{L}_{yx})\phi(x)$ is then defined to be the vector, $\phi(x)$, that was parallel transported along the curve $\mathscr{L}_{yx}$ to the point y, while $U(\mathscr{L}_{yx})$ is defined to be the parallel transporter. We require that every curve in space-time is associated with a parallel transporter in a manner that is both continuous and differentiable. This requires all parallel transporters to adhere to the following conditions.

1. $U(\emptyset) = \mathbf{1}$, i.e. a curve of length 0, denoted by $\emptyset$, must be represented by the unit matrix.

2. $U(\mathscr{L}_2 \circ \mathscr{L}_1) = U(\mathscr{L}_2)U(\mathscr{L}_1)$, in which the composition "$\mathscr{L}_2 \circ \mathscr{L}_1$" defines a path $\mathscr{L}_1$ followed by $\mathscr{L}_2$, such that the endpoint of $\mathscr{L}_1$ is the initial point of $\mathscr{L}_2$

3. $U(-\mathscr{L}) = U(\mathscr{L})^{-1}$, such that for a path travelled in the opposite direction, denoted by $-\mathscr{L}$, the parallel transporter is the inverse of the parallel transporter for the initial orientation.

These conditions ensure that under a local gauge transformation, as defined in eq. 2.2, the parallel transporter transforms as:

$$U(\mathscr{L}_{yx}) \to U'(\mathscr{L}_{yx}) = \Lambda(y)U(\mathscr{L}_{yx})\Lambda^{-1}(x) \tag{2.5}$$

The definition of the derivative requires the subtraction of two vectors located at points infinitesimally close to each other. We thus consider a straight curve from the point x to $x + \mathrm{d}x$. The parallel transporter that corresponds to this curve must deviate from the unit matrix by only an infinitesimal amount. We define it to be equal to

$$U(\mathscr{L}_{x+\mathrm{d}x,x}) = \mathbf{1} - A_\mu(x)\mathrm{d}x^\mu \tag{2.6}$$

in which A_μ is an element of $su(N)$, the Lie algebra corresponding to the group $SU(N)$, a vector space that consists of traceless, hermitian $N \times N$ matrices. We may now define the covariant differential of the vector $\phi(x)$ as

$$D\phi(x) = U^{-1}(\mathscr{L}_{x+\mathrm{d}x,x})\phi(x + dx) - \phi(x) \tag{2.7}$$

By noting that $D\phi(x) = D_\mu\phi(x)\mathrm{d}x^\mu$ we obtain the covariant derivative

$$D_\mu\phi(x) = (\partial_\mu + A_\mu(x))\phi(x) \tag{2.8}$$

The field $A_\mu(x)$ is now defined to be the gauge field and its transformation law may be derived from the transformation law of the parallel transporters:

$$A'_\mu(x) = \Lambda(x)A_\mu(x)\Lambda^{-1}(x) - (\partial_\mu\Lambda(x))\Lambda^{-1}(x) \tag{2.9}$$

$$= \Lambda(x)(\partial_\mu + A_\mu(x))\Lambda^{-1}(x) \tag{2.10}$$

Therefore the gauge field A_μ has been introduced as a connection. Finally the covariant derivative, under a local gauge transformation, transforms as

$$D'_\mu\phi'(x) = \Lambda(x)D_\mu\phi(x) \tag{2.11}$$

From the covariant derivative we may define the field strength $F_{\mu\nu}$. From a single point x we define a curve tracing an infinitesimal parallelogram with side lengths $\mathrm{d}x$ and $\mathrm{d}y$. The parallel transporter is then defined to be

$$U(\mathscr{L}) = 1 - F_{\mu\nu}(x)\mathrm{d}x^\mu\mathrm{d}y^\nu \tag{2.12}$$

It may be shown that this corresponds to the following definition for the field strength

$$F_{\mu\nu}(x) = [D_\mu, D_\nu] = \partial_\mu A_\nu(x) - \partial_\nu A_\mu(x) + [A_\mu(x), A_\nu(x)] \tag{2.13}$$

where the square brackets denote the commutator of the lie algebra $su(N)$. With this definition the field strength transforms under a local gauge transformation as

$$F'_{\mu\nu}(x) = \Lambda(x)F_{\mu\nu}\Lambda^{-1}(x) \tag{2.14}$$

As the Lie algebra $su(N)$ is by definition a vector space, all of its elements may be written as a linear combination of a set of basis vectors denoted by iT_a. Hence all elements X of the lie algebra may be written as:

$$X = \sum_{a=1}^{N} i\omega^a T_a \quad \omega^a \in \mathbb{R}$$

The matrices T_a are referred to as the generators of the lie algebra. The generators are embedded into matrices of a particular type which is dependent upon the representation of the algebra that is chosen, the most common of these being the fundamental and the adjoint representations. Regardless of the form of the embedding the algebra is defined by the relation

$$[T_a, T_b] = if_{abc}T_c \tag{2.15}$$

in which f_{abc} are the structure constants of the lie algebra. It may be shown that they are both antisymmetric and real. By definition the generators are traceless and hermitian, furthermore, they are usually normalized such that

$$\mathrm{Tr}\{T_a T_b\} = \frac{1}{2}\delta_{ab} \tag{2.16}$$

Using these definitions we rewrite the gauge field and the field strength in terms of component fields

$$A_\mu(x) = -igA^a_\mu(x)T_a \tag{2.17}$$

$$F_{\mu\nu}(x) = -igF^a_{\mu\nu}(x)T_a$$

The relationship between the gauge field and the field strength's component fields may be shown to be

$$F^a_{\mu\nu} = \partial_\mu A^a_\nu - \partial_\nu A^a_\mu + gf^{abc}A^b_\mu A^c_\nu \tag{2.18}$$

where g is referred to as the coupling constant. With the introduction of the covariant derivative we may now define a Lagrangian that is gauge invariant under a local $SU(N)$ gauge transformation:

$$\mathcal{L} = \phi(x)\cdot(D^\mu D_\mu + m^2)\phi(x) + U(\phi(x)\cdot\phi(x)) \tag{2.19}$$

This Lagrangian has introduced a new field, the gauge field A_μ. The dynamics of this field are giving by the Yang-Mills Lagrangian:

$$\mathcal{L}_{YM} = -\frac{1}{2}\,\mathrm{Tr}\{F_{\mu\nu}F_{\mu\nu}\} = -\frac{1}{4}F^a_{\mu\nu}F^a_{\mu\nu} \tag{2.20}$$

Quantum chromodynamics, and related theories, are the special cases in which the complex vector field is replaced with the Dirac spinor field that describes fermions of spin $\frac{1}{2}$, the complete Lagrangian of QCD like theories is thus given by

$$\mathcal{L} = -\frac{1}{4}F^a_{\mu\nu}F^a_{\mu\nu} + \bar{\psi}_i(i(\gamma^\mu D_\mu)_{ij} - m\delta_{ij})\psi_j \tag{2.21}$$

The fundamental microscopic degrees of freedom of QCD are quarks and gluons. The spectrum at low energy consists of meson, baryons, and glueballs. Glueballs themselves have hardly been determined experimentally because they mix with meson states. We are interested in determining the glueball states for large N Yang mills theories. As such we are not inerested in fermions and instead use the lagrangian given by equation 2.20.

The theory is then described by the partition function, the path integral over all field configurations:

$$Z = \int \mathcal{D}A\; e^{iS[A_\mu]} = \int \mathcal{D}A\; e^{i\int \mathrm{d}x^4 \mathcal{L}[A_\mu]} \tag{2.22}$$

while the expectation value of an operator $\mathcal{O}$ is given by

$$\langle \mathcal{O} \rangle = \frac{1}{Z}\int \mathcal{D}A\; \mathcal{O}\; e^{-S[A_\mu]} \tag{2.23}$$

3 Yang Mills Theory on a Lattice

By placing a Yang-Mills theory on a lattice effects certain features of the theories may be studied that are difficult to determine in the continuum case. One of the most prominent of these being the asymptotic freedom of QCD-like theories, which cannot be studied at low energy (IR) scales through pertubative techniques. A secondary benefit of using a lattice is that is may be easily represented and simulated on a computer. By discretizing the derivatives into finite differences, and the integrals into finite sums the problem is cast into the type of discrete mathematics that the binary nature of computers is particularly suited for.

When transferring a Yang-Mills theory onto a lattice several things need to occur. Firstly the lattice must be introduced, as such all points on the

lattice are separated by integer multiples of some lattice spacing a. This has the effect of producing a minimum distance (a) as well as a maximum momentum ($\frac{\pi}{a}$) on the lattice, discussed in more detail below. Secondarily, the path integral that describes the theory must undergo a Wick rotation such that is of a Boltzman form:

$$\int \mathcal{D}A \; e^{iS[A_\mu]} \rightarrow \int \mathcal{D}A \; e^{-S[A_\mu]} \tag{3.1}$$

This is necessary as computer simulations are exceedingly difficult to compute with complex valued integrals. The Boltzman term (e^{-S}) term in the path integral allows for the application of standard statistical techniques such as Markov Chain Monte Carlo simulations (see chapter 5).

Thirdly the derivatives and integrals must be discretized. As there exists a minimum distance between points, derivatives must be replaced with finite differences and integrals with finite sums. This requirement results in the introduction of a new action called the Wilson action that is discrete. It will be shown that the Wilson action coincides with the continuum Yang-Mills action described above in the limit of $a \rightarrow 0$.

Finally, the theory is placed in a finite volume. As computer simulations are not infinite only a finite number of points may be computed in any given simulation. As such lattices must be chosen to have a finite size usually represented with $R^3 \times T$ in which R is the number of lattice points along spacial axes and T the number of lattice points in the temporal axis. The finite volume demands that boundary conditions are to be placed upon the fields that act upon the lattice. The one used in this thesis is that of periodic boundary conditions, such that $\phi(x + R) = \phi(x)$ and $\phi(x + T) = \phi(x)$, in which ϕ is an arbitrary field and x is a space-time point.

3.1 Lattice and Discretization

We discretize space into a four dimensional hypercubical lattice. Of the four axes we let the three spatial axes has length R with a spacing between lattice elements a_s and the time axis have a length of T with a lattice spacing of a_t. In most cases we will also impose periodic boundary conditions on the lattice for bosonic fields. In the case of fermionic fields (not considered in this thesis) anti-periodic boundary conditions are applied. In the following we assume an isotropic lattice in which $a_s = a_t = a$.

The discrete nature of space requires redefinition of basic operators such

as the derivative and the integral. The forward derivative is defined to be

$$\Delta_\mu^f f(x) = \frac{1}{a}(f(x + a\hat{\mu}) - f(x)) \tag{3.2}$$

while the backwards derivative is defined to be

$$\Delta_\mu^b f(x) = \frac{1}{a}(f(x) - f(x - a\hat{\mu})) \tag{3.3}$$

We may note that both of these derivatives will converge to the continuous derivative ∂_μ in the limit of $a \to 0$. The two derivatives may be related to each other by

$$(\Delta_\mu^f)^\dagger = -\Delta_\mu^b \tag{3.4}$$

The integral over four dimensional space is redefined to be

$$\int \mathrm{d}x^4 f(x) \to \sum_x a^4 f(x) \tag{3.5}$$

where the sum is over all spacetime points on the lattice. We may note specifically that

$$\sum_x a^4 \ \Delta_\mu^f f(x) \ g(x) = -\sum_x a^4 f(x) \ \Delta_\mu^b g(x) \tag{3.6}$$

and further that

$$\sum_x a^4 \ \Delta_\mu^f f(x) \ \Delta_\mu^f f(x) = -\sum_x a^4 f(x) \ \Delta_\mu^b \Delta_\mu^f f(x) = \sum_x a^4 f \ \Box f \tag{3.7}$$

in which the Laplacian operator is defined as $\Box = -\Delta_\mu^b \Delta_\mu^f$. A more precise definition of how this operator acts on functions is given by the relation

$$\Box f(x) = \sum_{\mu=1}^{4} \frac{1}{a^2}(f(x) - f(x + a\hat{\mu}) - f(x - a\hat{\mu})) \tag{3.8}$$

Due to the fact that the lattice creates a UV cutoff for the theory this results in the Fourier transforms of functions defined on the lattice to be periodic with period $\frac{2\pi}{a}$ in momentum space. To see this let $\hat{f}(p)$ be a periodic function with period T, as $\hat{f}(p)$ is periodic it has a Fourier series representation

$$\hat{f}(p) = \sum_{n=-\infty}^{\infty} \hat{f}_n e^{2\pi i n p/T} \tag{3.9}$$

Computing the Fourier transform of this function

$$f(x) = \int_{-\infty}^{\infty} \hat{f}(p) e^{-ixp} \mathrm{d}p \tag{3.10}$$

$$= \sum_{n=-\infty}^{\infty} \hat{f}_n \int_{-\infty}^{\infty} e^{i(2\pi n/T - x)p} \mathrm{d}p = \sum_{n=-\infty}^{\infty} 2\pi \hat{f}_n \delta(x - 2\pi n/T) \tag{3.11}$$

Provided that we choose the period $T = \frac{2\pi}{a}$ the function $f(x)$ becomes a sum of delta functions evaluated at integer multiples of the lattice spacing a, i.e. discrete points on a lattice. Therefore, the momentum function $\hat{f}(p)$ must be periodic with period $\frac{2\pi}{a}$.

In addition, for all lattice points x, $\exp\{2\pi i x_\mu / a\} = 1$, therefore all momenta may be restricted to a limited region of momentum space, the first Brillouin zone, defined as

$$\mathcal{B} = \left\{ p | -\frac{\pi}{a} < p < \frac{\pi}{a} \right\} \tag{3.12}$$

As such the Fourier transform on the lattice takes the form

$$\int \frac{\mathrm{d}p^4}{(2\pi)^4} \to \int_{-\pi/a}^{\pi/a} \frac{\mathrm{d}p^4}{(2\pi)^4}$$

after the discretization of space-time. One of the consequences is that in that many of the integrations in loops, that in continuous space were zero, become finite on the lattice. All corrections that are dependent upon the lattice spacing a are called lattice artifacts, and must vanish in the continuum limit of $a \to 0$.

3.2 The Wilson Action

To derive a suitable action that is invariant under a local gauge transformation after the discretization of spacetime we take a set of similar steps as those in section 2. We once again begin by considering a matter field $\phi(x)$, which is now defined only for lattice points x. With corresponding generic action:

$$\mathcal{S} = \sum_x a^4 \phi(x) \cdot (\Box + m^2)\phi(x) + U(\phi(x) \cdot \phi(x)) \tag{3.13}$$

Similarly we define local gauge transformations $\Lambda(x)$ to be defined at points x only such that the transformation rule

$$\phi(x) \to \phi'(x) = \Lambda(x)\phi(x) \tag{3.14}$$

continues to hold true on lattice points. Examining the kinetic part of the action we may notice that using the definitions of the forward derivative it may be rewritten in the form [15]

$$\frac{1}{2}\sum_x a^4 \Delta^f_\mu \phi \cdot \Delta^f_\mu \phi = -\sum_{<xy>} a^2 \phi(x)\cdot\phi(y) + 4\sum_x a^4 \phi(x)\cdot\phi(x) \tag{3.15}$$

in which $< xy >$ represents the set of all nearest neighbor points. Examining equation 3.15 we may note that while the second term on the right hand side is gauge invariant, the nearest neighbor term is not. As such we must once again introduce a covariant derivative and corresponding gauge field. In the continuum case, a parallel transporter is defined through the infinitesimal difference between neighboring points. On the lattice all distances must have a minimum distance equal to the lattice spacing a, as such the corresponding parallel transporters are based on the links b between neighboring lattice sites. If we let x represent some point on the lattice, and let $x + a\hat{\mu}$ be a neighboring point in the direction of $\hat{\mu}$ (where $\hat{\mu} = 1, 2, 3, 4$, representing the four lattice axes), we define a link b to be the directed straight line (or path) between these two points represented by

$$b =< x + a\hat{\mu}, x >\equiv (x, \mu) \tag{3.16}$$

As in the continuous case we define the parallel transporter, which is an element of the local gauge group G, as a matrix associated to an individual link denoted as

$$U(b) \equiv U(x + a\hat{\mu}, x) \equiv U_{x\mu} \tag{3.17}$$

By convention this is usually referred to as a link variable. When considering an arbitrary path on the lattice consisting of a number of links

$$\mathscr{L} = b_n \circ \cdots \circ b_2 \circ b_1 \tag{3.18}$$

the parallel transporter is defined to be

$$U(\mathscr{L}) = U(b_n)\ldots U(b_1) = \prod_{b\in\mathscr{L}} U(b) \tag{3.19}$$

By the properties of a parallel transporter, for a path connecting points x and y, U must satisfy.

$$U(y, x) = U^{-1}(x, y) \tag{3.20}$$

We now define the set of all link variables $\{U(b)\}$ to be the gauge field on the lattice. These link variables transform, under a gauge transformation, as continuum parallel transporters

$$U'(x, y) = \Lambda(x)U(x, y)\Lambda^{-1}(y) \tag{3.21}$$

which implies that the nearest neighbor coupling term in the action will be locally gauge invariant in the form

$$\sum_{<xy>} \phi(x) \cdot U(x,y)\phi(y) \tag{3.22}$$

Equivalently, a covariant forwards derivative may also be defined as

$$D_\mu \phi = \frac{1}{a}\left(U^{-1}(x,\mu)\phi(x+a\hat{\mu}) - \phi(x)\right) \tag{3.23}$$

such that the kinetic field term takes the form

$$\frac{1}{2}\sum_x a^4 D_\mu\phi \cdot D_\mu\phi = -\sum_{<xy>} a^2\phi(x)\cdot U(x,y)\phi(y) + 4\sum_x a^4\phi^2(x) \tag{3.24}$$

In either case it becomes apparent that gauge invariant quantities may be constructed from elements of the form

$$\phi(x)\cdot U(\mathscr{L}_{x,y})\phi(y) \tag{3.25}$$

In order to determine the gauge invariant Wilson action we use operators of this type, with the various paths chosen to be plaquettes. Plaquettes are the smallest closed curves on the lattice consisting of the links between four nearest neighbor lattice points forming a square. For a lattice point x an example plaquette would contain the points

$$x \quad x+a\hat{\mu} \quad x+a\hat{\mu}+a\hat{\nu} \quad x+a\hat{\nu} \tag{3.26}$$

in which both a $\hat{\mu}$ and $\hat{\nu}$ are unit vectors pointing along one of the 4 lattice axes with $\hat{\mu} \neq \hat{\nu}$. Plaquettes also have orientations, and maybe traversed in two different ways, with the convention being that counterclockwise traversal is positive. A plaquette is denoted by $p = (x;\hat{\mu},\hat{\nu})$, with the parallel transporter of the plaquette defined as

$$\begin{aligned} &U_p \equiv U_{x;\mu\nu} \equiv \\ &U(x,x+a\hat{\mu})U(x+a\hat{\mu},x+a\hat{\mu}+a\hat{\nu})U(x+a\hat{\mu}+a\hat{\nu},x+a\hat{\nu})U(x+a\hat{\nu},x) \end{aligned} \tag{3.27}$$

and is called the plaquette variable. The plaquette variable corresponding to the opposite orientation of the plaquette is simply the inverse U_p^{-1}. The Wilson action is defined in terms of plaquette variables to be

$$S[U] = \sum_p S_p(U_p)$$

where the sum is defined to be over all plaquettes, with only one of the two orientations, ie.

$$\sum_p \equiv \sum_x \sum_{1\leq\hat{\mu}<\hat{\nu}\leq 4}$$

And the plaquette term S_p (in the case of $SU(N)$) is given by

$$S_p(U) = -\beta\left\{\frac{1}{2\,\mathrm{Tr}\,\mathbf{1}}\left(\mathrm{Tr}\,U + \mathrm{Tr}\,U^{-1}\right) - 1\right\} = \beta\left\{1 - \frac{1}{N}\,\mathrm{Re}\,\mathrm{Tr}\,U\right\} \quad (3.28)$$

where β is a parameter related to the inverse of the coupling constant, to be defined later. The constant term of is often left out as it is physically insignificant [15]. Furthermore the Wilson action is real and gauge invariant due to the fact that

$$\mathrm{Tr}\,U_p' = \mathrm{Tr}\,U_p \quad (3.29)$$

It is now necessary to show that the Wilson action will coincide with the continuum Yang-Mills action in the limit of $a \to 0$, with corrections of order $\mathcal{O}(a)$. We first define a gauge field A_μ as in the continuum case, as a vector field of the Lie algebra corresponding to the Lie group. We let

$$A_\mu(x) = -igA_\mu^b(x)T_b \quad (3.30)$$

and then let

$$U(x,\mu) \equiv e^{-aA_\mu(x)} = 1 - aA_\mu(x) + \frac{a^2}{2}A_\mu^2(x) + \ldots \quad (3.31)$$

As we are considering the $a \to 0$ limit higher order a terms may be ignored. Using the Campbell-Baker-Hausdorff formula, which states that

$$e^x e^y = e^{x+y+(1/2)[x,y]+\cdots} \quad (3.32)$$

and the fact that on the lattice

$$A_\nu(x + a\hat{\mu}) = A_\nu(x) + a\Delta_\mu^f A_\nu(x) \quad (3.33)$$

we may determine that

$$U_p = U_{x;\mu\nu} = \exp -a^2 G_{\mu\nu}(x) \quad (3.34)$$

in which

$$G_{\mu\nu}(x) = F_{\mu\nu}(x) + \mathcal{O}(a) \quad (3.35)$$

with $F_{\mu\nu}$ the field strength on the lattice defined as

$$F_{\mu\nu}(x) = \Delta^f_\mu A_\nu(x) - \Delta^f_\nu A_\mu(x) + [A_\mu(x), A_\nu(x)] \tag{3.36}$$

Since by the properties of an $su(n)$ Lie algebra

$$\mathrm{Tr}(G_{\mu\nu}(x)) = 0 \tag{3.37}$$

this results in the fact that

$$\mathrm{Tr}\Big(U_p + U_p^{-1}\Big) = 2\,\mathrm{Tr}\,\mathbf{1} + a^4\,\mathrm{Tr}(F_{\mu\nu})^2 + \mathcal{O}(a^5) \tag{3.38}$$

Finally using the definition of the plaquette sum

$$\sum_p \mathrm{Tr}(F_{\mu\nu})^2 = \frac{1}{2}\sum_{x,\mu,\nu} \mathrm{Tr}(F_{\mu\nu})^2 \tag{3.39}$$

The Wilson action may equivalently be represented as

$$S = -\frac{\beta}{4N}\sum_x a^4\,\mathrm{Tr}\,F_{\mu\nu}(x)F^{\mu\nu} + \mathcal{O}(a^5) \tag{3.40}$$

showing that in the limit of $a \to 0$, the Wilson action will converge on to the Yang-Mills action provided that we select

$$\beta = \frac{2N}{g^2} \tag{3.41}$$

in which g is the bare coupling constant.

Similarly to the continuum case the theory is now describe the the path integral:

$$Z = \int \mathcal{D}U\ e^{-S[U]} \tag{3.42}$$

in which $U \equiv \{U(b)\}$, the configuration of all link variables on the lattice. The measure $\mathcal{D}U$ is the Haar measure on the gauge group which guarantees invariance and normalization. Observables on the lattice are functions of the configuration of link variable, U,

$$\mathcal{O}(\{U(b)\}) \equiv \mathcal{O}(U) \tag{3.43}$$

with the expectation value of an observable being given by

$$\langle\mathcal{O}\rangle = \frac{1}{Z}\int \mathcal{D}U\ \mathcal{O}e^{-S[U]} \tag{3.44}$$

4 Glueball Operator States

The existence of glueballs were first proposed as theoretical particles in the early in 1970s by H. Fritzsch and M. Gell-Mann [16]. These particles were proposed to consist of gluons, the force carrying particles of the strong force, created throught the field's interaction with itself. The physical existence of glueballs has not yet been confirmed through particle accelerator experiments although a large number of candidates exist (see for example [9, 8]).

The purpose of this thesis is to determine the mass spectrum of glueball particles. The massive particles are denoted primarily by their spin J as well as their parity P and charge parity C, denoted as J^{PC}. To determine the mass of any of these glueballs the euclidean correlator must be determined, defined as

$$\langle\psi(t)\psi(0)\rangle_T = \frac{1}{\int \mathcal{D}U\ e^{-S}} \int \mathcal{D}U\ e^{-S}\psi(t)\psi(0) \tag{4.1}$$

In which ψ is a glueball operator given by a function with the parameter t denoting the time-plane of the lattice on which it is evaluated, T is the size of the lattice in the time direction. Alternatively we may express this relation with

$$\langle\psi(t)\psi(0)\rangle_T = \frac{1}{Z}\,\mathrm{Tr}\left[e^{-(T-t)\hat{H}}\hat{\psi}e^{-t\hat{H}}\hat{\psi}\right] \tag{4.2}$$

In which $\hat{\psi}$ are creation and destruction operators of glueballs, $\hat{H}$ is the Hamiltonian of the system. The operator $e^{-t\hat{H}}$ is called the transfer matrix, connects spacelike planes separated by a distance of t. In this formalism Z is represented by:

$$Z = \mathrm{Tr}\left[e^{-T\hat{H}}\right] \tag{4.3}$$

In order to relate this equation to the mass gap of the operator ψ we evaluate the trace on a basis of the eigenstates of the Hamiltonian $|n\rangle$, on which $\hat{H}\,|n\rangle = E_n\,|n\rangle$, in which E_n is the energy, which is real and ordered such that E_0 is the lowest and represents the energy of the vacuum.

$$Z = \sum_n \langle n|\, e^{-T\hat{H}}\, |n\rangle = \sum_n e^{-TE_n} \tag{4.4}$$

The correlator itself may be similarly expressed as

$$\langle\psi(t)\psi(0)\rangle_T = \frac{1}{Z}\sum_{m,n}\langle m|\, e^{-(T-t)\hat{H}}\hat{\psi}\,|n\rangle\,\langle n|\, e^{-t\hat{H}}\hat{\psi}\,|m\rangle \tag{4.5}$$

$$= \frac{1}{Z}\sum_{m,n} e^{-(T-t)E_m}\,\langle m|\,\hat{\psi}\,|n\rangle\, e^{-tE_n}\,\langle n|\,\hat{\psi}\,|m\rangle \tag{4.6}$$

$$= \frac{\sum_{m,n}\langle m|\,\hat{\psi}\,|n\rangle\,\langle n|\,\hat{\psi}\,|m\rangle\, e^{-t\Delta E_n}e^{-(T-t)\Delta E_m}}{1+e^{-T\Delta E_1}+e^{-T\Delta E_2}+\cdots} \tag{4.7}$$

in which we have defined $\Delta E_n = E_n - E_0$ in the final step. We now examine the correlator in the limit of $T \to \infty$. In this limit it is obvious that the denominator reduces to 1, while in the numerator all terms in which $\Delta E_m \neq 0$ become 0. As such we end up with the relation

$$\langle\psi(t)\psi(0)\rangle = \sum_n \langle 0|\,\hat{\psi}\,|n\rangle\,\langle n|\,\hat{\psi}\,|n\rangle\, e^{-t\Delta E_n} \tag{4.8}$$

When t is large all terms of ΔE_n except for ΔE_0 may be ignored. As this value ΔE_0 is the difference in energy between the vacuum and the lowest glueball state it is equivalent to the mass m that we wish to determine, as such

$$\langle\psi(t)\psi(0)\rangle \simeq Ce^{-tm} \tag{4.9}$$

In which C is a constant. However, in the case of periodic boundary conditions on the Yang-Mills field the term with $e^{-(T-t)m}$ also survives resulting in

$$\langle\psi(t)\psi(0)\rangle \simeq C(e^{-tm}+e^{-(T-t)m}) \tag{4.10}$$

As such in order to determine the glueball masses we need a method to measure the correlators on the lattice. This first requires a means of expressing a glueball wavefunction $|\psi\rangle$ on the lattice. We require that the glueball wavefunctions are orthogonal to the vacuum, $\langle 0|\psi\rangle = 0$. In this case, we may note that if we have a complete set of gauge-invariant operators, denoted by F_i where i is an integer, that satisfy the relation $\langle 0|\,F_i\,|0\rangle = 0$ we may represent a generic wave function as a linear combination of the operators

$$|\psi\rangle = \sum_i c_i F_i\,|0\rangle \tag{4.11}$$

in which c_i are complex constants. A Wilson loop is an ordered collection of links on the lattice that form a closed group. By choosing the set F_i to be

products of sets of spacelike Wilson loops in the various representations of the $SU(N)$ group,

$$O_{i,v}(\mathbf{x},t) = \chi_v(\prod_{C_i} U) - \langle 0|\chi_v(\prod_{C_i} U)|0\rangle \tag{4.12}$$

a suitable basis for expressing glueball wavefunctions may be obtained [17]. In this equation i represents the the ith closed curve Wilson loop C_i and v gives the representation of the SU(N) group. χ_v is the character of the representation v. For the coordinates of the loop we take $\mathbf{x}$ to be the mathematical center and t to be the time slice on which the operator resides. This thesis seeks to find the lowest energy states of the glueball spectrum, as such we ignore states with momentum $\mathbf{p} \neq 0$. Our set of operators F_i, which we now denote by $O_{i,v}$, is chosen to be

$$O_{i,v}(t) = \sum_{\mathbf{x}} O_{i,v}(\mathbf{x},t) \tag{4.13}$$

To obtain the glueball mass spectrum we must determine the operators, or linear combinations of operators, $O_{i,v}$ which correspond to the glueball particles states of particular spin, parity, and charge parity.

Particles with a given spin are embedded in representations of the n-dimensional rotational group. One the lattice however, rotational symmetry is broken, and only restored in the continuum limit. The lattice has cubic symmetry. The cubic symmetry is discrete in the number of elements and has only 5 representations. Hence all rotational symmetry representations subduced onto the lattice must be constructed from linear combination of cubic symmetry representations, such that in the continuum limit, the correct rotational symmetry representation is restored [18].

4.1 The Cubic symmetry group

The symmetry group of the cube, O, consists of 24 elements divided into 5 conjugacy classes. Each of these elements represents a transformation of the cube in which the cube is rotated around an axis. The first element of the group is the identity in which nothing is changed denoted by 1.

There are three axes that may be drawn perpendicular to the faces of the cube. Around each of these axes 4 rotations might occur in increments of 90 degrees. These are denoted by $C_4^{(i)}$, (i = 1, 2, 3). The index i represents which of the three axes is chosen, the 90 degree rotations are represented by $C_4^{(i)}, (C_4^{(i)})^2, (C_4^{(i)})^3, (C_4^{(i)})^4 = 1)$. See figure 4.1a.

There are 4 axes connecting two of vertices of the cube such the axis passes through the center of the cube. Around these axes the cube may be rotated 3 times in increments of 120 degrees. These elements are denoted by $C_3^{(i)}$, (i = 1, 2, 3, 4). See figure 4.1b.

There are 6 axes connecting the center of two edges of the cube such that the axis passes through the center of the cube. Around each of these axis two rotations may occur, in increments of 180 degrees. These elements are denoted by $C_2^{(i)}$, (i = $1, \ldots, 6$). See figure 4.1c (note that only 3 of the axes are shown in the image for clarity).

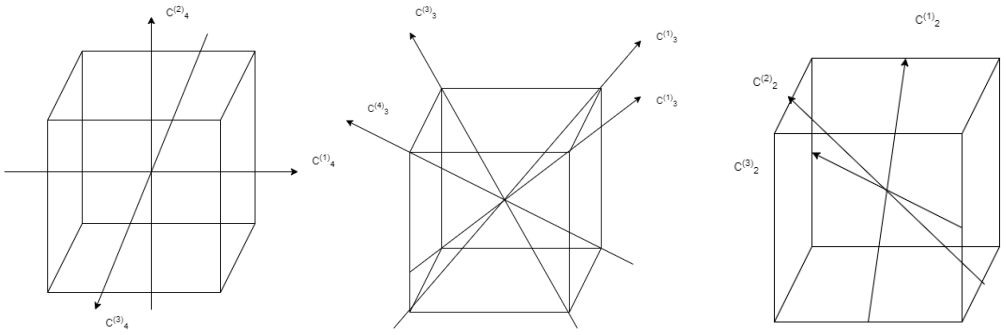

(a) C4 (b) C3 (c) C2

Figure 4.1: The axes of rotation for the C4, C3, and C2 element classes of the cubic symmetry group. For C2 only 3 of the total of 6 rotational axes are shown for clarity

These 24 elements are given in coordinate form in table 4.1.

The 5 conjugacy classes[1] are represented by E, C_4, C_4^2, C_3, and C_2. Their elements are

$$E = \{1\} \quad C_4 = \{C_4^{(i)}\} \quad C_4^2 = \{(C_4^{(i)})^2\} \tag{4.14}$$

$$C_3 = \{, C_3^{(i)}, (C_3^{(i)})^2\} \quad C_2 = \{C_2^{(i)}\} \tag{4.15}$$

These 5 classes correspond to the fact that there exist five irreducible representations of the group. The Burnside theorem states that the square of the dimensions of the representations must sum to the number of group elements, in the present case this gives dimensions of 1, 1, 2, 3, 3. These

[1]Two elements $a, b \in G$ of a group G are conjugate if $b = g^{-1}ag$ for some $g \in G$. The conjugacy class of an element a is defined to be $Cl(a) = \{g^{-1}ag | g \in G\}$

Index	Operation	Index	Operation
1	$(x, y, z) \to (x, y, z)$	13	$(x, y, z) \to (-z, y, x)$
2	$(x, y, z) \to (-z, -y, -x)$	14	$(x, y, z) \to (-x, -y, z)$
3	$(x, y, z) \to (z, x, y)$	15	$(x, y, z) \to (-y, x, z)$
4	$(x, y, z) \to (-y, -x, -z)$	16	$(x, y, z) \to (-z, -x, y)$
5	$(x, y, z) \to (y, z, x)$	17	$(x, y, z) \to (-x, z, y)$
6	$(x, y, z) \to (-x, -z, -y)$	18	$(x, y, z) \to (-y, -z, x)$
7	$(x, y, z) \to (-x, -z, y)$	19	$(x, y, z) \to (-x, y, -z)$
8	$(x, y, z) \to (x, -y, -z)$	20	$(x, y, z) \to (z, -y, x)$
9	$(x, y, z) \to (y, x, -z)$	21	$(x, y, z) \to (-z, x, -y)$
10	$(x, y, z) \to (z, -x, -y)$	22	$(x, y, z) \to (y, -x, z)$
11	$(x, y, z) \to (x, z, -y)$	23	$(x, y, z) \to (-y, z, -x)$
12	$(x, y, z) \to (y, -z, -x)$	24	$(x, y, z) \to (x, -z, y)$

Table 4.1: The set of 24 operations that define the O symmetry group of the cube as represented in coordinate transformations

	E	$6C_2$	$8C_3$	$6C_4$	$3C_4^2$
A_1	1	1	1	1	1
A_2	1	-1	1	-1	1
E	2	0	-1	0	2
T_1	3	-1	0	1	-1
T_2	3	1	1	-1	-1

Table 4.2: Character table for the conjugacy groups of the cubic group. Each column gives the character of that columns conjugacy class in the rows representation of the group.

5 irreducible representations are denoted as A_1, A_2, E, T_1, T_2. Of these A_1 is the trivial representation and T_1 is the standard vector representation. The representations have equivalent character for all elements within one conjugacy group, these characters are listed in table 4.2

The parity is group P is a simple group consisting of two elements $P = \{1, -1\}$. The direct product of the cubic group O together with the parity group P is called O_h and includes the rotations of the O group but also reflections and inversions through the cubes center. All elements of the O_h group are of the form $g_h = g \times 1$ or $g_h = g \times -1$ for all $g \in O$. This doubles the number of conjugacy groups to 10, represented by $A_1^{\pm}, A_2^{\pm}, E^{\pm}, T_1^{\pm}, T_2^{\pm}$. The + symbol corresponds to the fact that the characters of group elements

under the representation follow $\chi(1 \times g) = \chi(-1 \times g)$, while representations denoted with the $-$ sign follow the rule $\chi(1 \times g) = -\chi(-1 \times g)$.

The charge conjugacy operator operates similarly to the parity operator increasing the total size of the group in question to 96 elements, with 20 conjugacy classes. These 20 representations will be denoted by R^{PC}, in which $R = A_1, A_2, E, T_1, T_2$, and $P = \pm$, $C = \pm$.

4.2 Spin states with respect to the cubic group

In the continuum limit of the lattice gauge theory rotational invariance is restored. Selection rules for particles must therefore be dependent on the irreducible representations of the rotation group. The wave functions that describe states of spin J that belong to the irreducible representation D_J will be represented by $|\psi\rangle_J$. We focus only on integer spins during this discussion and ignore parity and charge parity, for the sake of clarity.

On the lattice, for all values of β, an exact cubic symmetry is present. This implies that selection rules must follow from the 5 irreducible representations of the cubic group O. We denote these states as $|\psi\rangle_R$, in which R is one of the representations discussed above (see table 4.2).

This implies that in the continuum limit of $\beta \to \infty$ all cubic states should be expressed in terms of states with spin J. More explicitly

$$|\psi\rangle_R = \sum_{J,m} c^R_{J,m} |\psi\rangle_{J,m} \tag{4.16}$$

In which m is the quantum number that corresponds to the z component of the spin vector, that may take values from $-J, -J+1, \ldots, J-1, J$. From this we may note that a wavefunction of spin J may only contribute to the wavefuntion of a cubic representation R if

$$D^0_J \supset R \tag{4.17}$$

In which D^0_J is the subduced representation of the representation D_J which is obtained by embedding the cubic group into the rotation group. This subduced representation of the rotational group has been computed by many authors previously [19]. Table 4.3 which gives the multiplicities of the cubic representations R which are found within each subduced representation D^0_J up until a spin of $J = 6$.

From this we may note that for spins $J > 1$ the subduced representations are reducible and all representations of the cubic group have appeared by

R | J	0	1	2	3	4	5	6
A_1	1	0	0	0	1	0	1
A_2	0	0	0	1	0	0	1
E	0	0	1	0	1	1	1
T_1	0	1	0	1	1	2	1
T_2	0	0	1	1	1	1	2

Table 4.3: Multiplicities of cubic representations in the subduced representation D^0_J of spin J

spin $J = 3$. Extensions of this analysis to half-integer spin also exist and may be found in [20].

Now we consider the definition of the mass given by equation 4.10 and restrict ourselves to states $|\psi\rangle_R$ with the condition $\langle 0|\psi\rangle_R = 0$. We let the eigenvalues be denoted by $m(R)$. Now provided that we operate under the assumption: that the eigenvalue $m(R)$ corresponds to the lowest allowed spin in the sector $|\psi\rangle_R$ [17]; we may then read from table 4.3 that in the continuum limit:

$$m(0^{PC}) = m(A_1^{PC}) \tag{4.18}$$

$$m(1^{PC}) = m(T_1^{PC}) \tag{4.19}$$

$$m(2^{PC}) = m(E^{PC}) = m(T_2^{PC}) \tag{4.20}$$

$$m(3^{PC}) = m(A_2^{PC}) = m(T_1^{PC}) = m(T_2^{PC}) \tag{4.21}$$

It is important to note that these relations only hold true in the continuum limit, specifically when $\beta = \infty$. During the simulations we must choose a value of β for which the relationship is approximately true. Due to the fact that we are estimating the lowest energy eigenvalue $m(R)$ of the wavefunctions $|\psi\rangle_R$ we are limited to determining the properties of particles with spin $J \leq 3$.

4.3 Irreducible cubic group representations and corresponding Wilson loops

We now wish to construct a set of Wilson loops that correspond to irreducible representations of the cubic symmetry group O_h. By constructing these irreducible representations onto closed Wilson loops, we may use the linear combinations of Wilson loop operators as glueball states with representation R^{PC}. As seen in the previous section the mass of these operators will be equivalent to continuum glueballs with spin J^{PC}. As such on the lattice

we can measure the correlations between closed Wilson loops to determine glueball mass.

It will be shown that all representations may be constructed with Wilson loops of length 8 or less, in which the length is the number of links which the loops consists of. All spacelike Wilson loops up till and including length 8 may be seen in figure 4.2. Note that all of these loops have various spatial orientations under transformations of the cubic symmetry group. For example, the plaquette may be in the XY, XZ, or YZ plane.

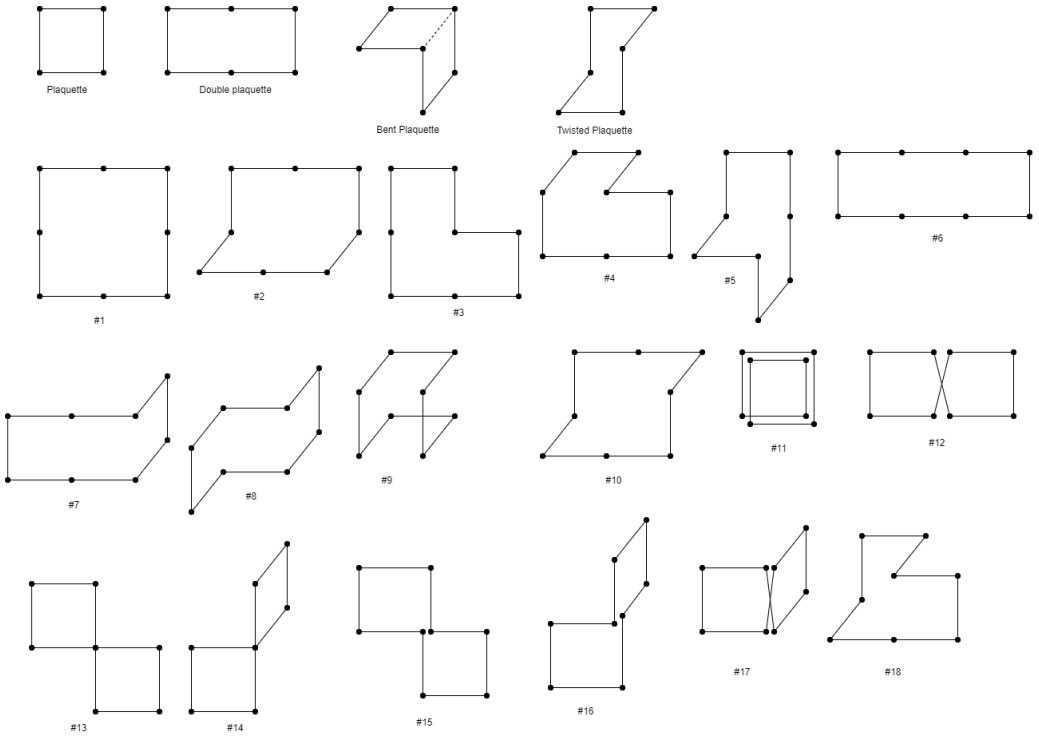

Figure 4.2: All closed Wilson loops up to length 8. The first row are common enough loops that they are named. All loops of length 8 are designated a number from 1 to 18. All loops have a number of spatial orientations under transformation of the cubic symmetry group.

Due to the fact that for $N \geq 3$ the $SU(N)$ links have a character that is complex, the Wilson loops will have an orientation of traversal depending on the order of the multiplication of the links. By convention, we choose counterclockwise to be the positive orientation. We note that in the continuum, the gauge field in the lagrangian transforms under charge parity in the

following manner:

$$A_\mu \xrightarrow{C} -A_\mu^T \tag{4.22}$$

provided that the gauge field is hermitian. This allows us to determine an important rule of the Wilson loop operators: the real part of the character of a Wilson loop has charge parity $C = 1$ while the imaginary part has charge parity $C = -1$. As $SU(2)$ has no orientation, in $S(2)$ all $C = -1$ results may be ignored entirely.

We now consider Wilson loop operators $O_{i,v}$ of length L. In the construction of these operators only the shape of the loop and its orientation is important, as such we denote the loop as a tuple of length L:

$$(\hat{f}_1, \ldots, \hat{f}_L) \qquad \sum_{i=1}^{L} \hat{f}_i = 0 \tag{4.23}$$

In this representation the $\hat{f}_i$ are vectors drawn from the set of positive and negative spatial unit vectors, $\hat{f}_i \in \{\pm\hat{e}_j | j = 1, 2, 3\}$. Under this notation, the simplest Wilson loop, the spatial plaquette in the XY plane in positive orientations would be represented by $(\hat{e}_1, \hat{e}_2, -\hat{e}_1, -\hat{e}_2)$ while the opposite orientation is given by $(\hat{e}_2, \hat{e}_1, -\hat{e}_2, -\hat{e}_1)$. Note that because the loops are closed, two cyclic permutations of the tuples are identical. As such the tuples form an equivalence class. The equivalence class of the tuple $(\hat{f}_1, \ldots, \hat{f}_L)$ is denoted by $[\hat{f}_1, \ldots, \hat{f}_L]$. We now consider the effect of charge conjugation on these equivalence classes noting that

$$C[\hat{f}_1, \ldots, \hat{f}_L] = [-\hat{f}_L, -\hat{f}_{L-1}, \ldots, -\hat{f}_1] \tag{4.24}$$

We may construct a set of operators that have positive or negative C-parity by considering operators $O_{i,v}^{\pm}$ constructred from the combinations:

$$[\hat{f}_1, \ldots, \hat{f}_L]_\pm = [\hat{f}_1, \ldots, \hat{f}_L] \pm [-\hat{f}_L, \ldots, -\hat{f}_1] \tag{4.25}$$

It is clear that $C[\hat{f}_1, \ldots, \hat{f}_L]_\pm = \pm[\hat{f}_1, \ldots, \hat{f}_L]_\pm$.

We now generate a representation $\mathcal{M}$ of the cubic group O_h. For each element $g \in O_h$ we apply $\mathcal{M}_g$ on the fixed shape operators $O_{i,v}^{\pm}$ by:

$$\mathcal{M}_g[\hat{f}_1, \ldots, \hat{f}_L]_\pm = [M_g\hat{f}_1, \ldots, M_g\hat{f}_L] \tag{4.26}$$

here M_g is defined to be the matrix that corresponds to g in the vector representation on the basis $(\hat{e}_1, \hat{e}_2, \hat{e}_3)$. The collection of all $\mathcal{M}_g$ form the representation $\mathcal{M}$.This generated representation $\mathcal{M}$ will have dimension of

OP	d	A_1^{++}	A_2^{++}	E^{++}	T_1^{++}	T_2^{++}	A_1^{+-}	A_2^{+-}	E^{+-}	T_1^{+-}	T_2^{+-}
p^*	6	1	0	1	0	0	0	0	0	1	0
dp	12	1	1	2	0	0	0	0	0	1	1
bp	24	1	0	1	0	1	0	0	0	1	1
tp	8	1	0	0	0	1	0	1	0	1	0
		A_1^{-+}	A_2^{-+}	E^{-+}	T_1^{-+}	T_2^{-+}	A_1^{--}	A_2^{--}	E^{--}	T_1^{--}	T_2^{--}
bp	24	0	0	0	1	1	1	0	1	0	1

Table 4.4: Multiplicities of irreducible representations of the cubic group $O_h \times C$ in the representation $\mathcal{M}$ or various operators of length 6 or below. * p = plaquette, dp= double plaquette, bp = bent plaquette, tp = twisted plaquette, see figure 4.2

less than or equal to 96. This number comes from the number of elements in O_h (48) with the direct produce with charge parity C (2). As previously mentioned, in $SU(2)$ the $C = 1$ and $C = -1$ results are equivalent, as such the dimension of the representation $\mathcal{M}$ has a maximum size of 48.

The representation matrices of individual group elements g, $\mathcal{M}_g$ are $d \times d$ matrices where all entries are either 1, 0, or -1. The lowest dimension is for the plaquette in which $d = 6$, which corresponds to the three spacial orientations, XY plane, YZ plane, and XZ plane, and the two traversal orientations (clockwise and counterclockwise).

We will determine the multiplicity of irreducible representations of the cubic group in the representation $\mathcal{M}$ constructed upon the closed Wilson loop. This may be completed by means of the character relation. For a fixed charge parity, C either $+1$ or -1, the multiplicity m_{R^P} of the representation R^P in the irreducible representation decomposition of the representation $\mathcal{M}$ is given by:

$$m_{R^P} = \frac{1}{48} \sum_K n_K \chi_K^{\mathcal{M}} \chi_K^{R^P} \tag{4.27}$$

in which K are the conjugacy classes of the group O_h. Each conjugacy class has a number of elements n_K. $\chi_K^{\mathcal{M}}$ is the character of $\mathcal{M}$ for any element of the conjugacy class K, similarly $\chi_K^{R^P}$ is the character of any element of the conjugacy class K of the representation R^P. The multiplicities for the representation for all Wilson operators up to length 6 may be seen in table 4.4, a table with multiplicities for operators up to length 8 may be found in the appendix (see tables A.1, A.2). As may be seen from these tables all irreducible representations are present in Wilson loops up to a length of 8.

	O_1	O_2	O_3
A_1^{++}	1	1	1
E^{++}	0	1	-1
	-2	1	1
T_1^{+-}	1	0	0
	0	1	0
	0	0	1

Table 4.5: Wavefunctions for various glueball states that may be constructed from the plaquette operator. For definition of O_i see figure B.1

The final step in this process is to use the information about the irreducible content of each representation in $\mathcal{M}$ to produce orthonormal basis for each representation R^P explicitly. The method used in this thesis is one used by Berg and Billiore[17]. We let C equal to a matrix that commutes with all $\mathcal{M}_g$ of the representation $\mathcal{M}$. We then let A equal to the matrix that diagonalizes C, in the sense that ACA^{-1} is a diagonal matrix, then the matrix A will also reduce the representation $\mathcal{M}$ although not necessarily completely. In subsequent steps one may then use the representation

$$A\mathcal{M}A^{-1} = \{A\mathcal{M}_g A^{-1} | \mathcal{M}_g \in \mathcal{M}\} \tag{4.28}$$

The matrices C that commute with all elements of $\mathcal{M}$ may be constructed by summing all of the matrices of a single conjugacy class of $\mathcal{M}$. The orthonormal bases may be read off from the columns of the matrices A. Using this method, the representations may be fully reduced with only a few conjugacy classes. In tables 4.5 and 4.6 we represent the orthonormal bases for representations constructed from the plaquette operator and the double plaquette operator, additional operators may be found in the appendix (see appendix B). The columns in the table represent the various spacial orientations of the operator, three in the case of the plaquette, 6 for the double plaquette, figures showing these spatial orientations may be found in appendix B. As such from table 4.5 we see that the A_1^{++} glueball may be represented with the real part of the operator $O_1 + O_2 + O_3$, or the sum of the three spatial orientations of the plaquette. Furthermore the case of $C = \pm$ the real or imaginary part of the operator has to be taken to correspond to the C-parity. Normalization factors are also not included.

	O_1	O_2	O_3	O_4	O_5	O_6
A_1^{++}	1	1	1	1	1	1
A_2^{++}	1	1	1	-1	-1	-1
E^{++}	0	1	-1	0	1	-1
	-2	1	1	-2	1	1
E^{++}	-2	1	1	2	-1	-1
	0	-1	1	0	1	-1
T_1^{+-}	1	0	0	1	0	0
	0	1	0	0	1	0
	0	0	1	0	0	1
T_2^{+-}	1	0	0	-1	0	0
	0	1	0	0	-1	0
	0	0	1	0	0	-1

Table 4.6: Wavefunctions for various glueball states that may be constructed from the double plaquette operator. For definition of O_i see figure B.2

5 Numerical Simulation Details

To measure the value of an observable $\mathcal{O}$ on the lattices requires the evaluation of the euclidian path integral

$$\langle \mathcal{O} \rangle = \frac{1}{Z} \int \mathcal{D}U \ \mathcal{O}[U] e^{-S[U]} \tag{5.1}$$

We have introduced the lattice to find a non perturbative solution and aim to solve it using a computer simulation. However, it may not be solved numerically because the number of states that would have to be calculated would be infinite. For example, in the simplest possible case of the Ising model, in which each link can take a binary value of either 1 or -1, with N links this would require the computation of 2^N states. In the present case in which the link U are of the type $SU(N)$ this number is far greater. As such an alternative method is required to approximate the integral, for this problem we make use of a Monte-Carlo method. We approach the problem statistically. Instead of generating all possible configurations we draw individual configurations $[U]$ from a probability distribution to form a representative sample of configurations, measurements upon which approximate the true values of $\langle \mathcal{O} \rangle$.

The Boltzman factor, $\exp\{-S[U]\}$ is of particular importance. We may note that the action S includes a term which sums over the entire lattice. Considering the total number of lattice points to be Ω, for illustrative purposes we may rewrite the action as $S[U] = \Omega s[U]$, in which $s[U]$ is the density of the action. As the value of Ω is large in any reasonable lattice used for measurement this exponential factor is small except for in a small range around the minimum energy density. For the sake of efficiency, an effective Monte-Carlo algorithm must consider this factor and draw random field configurations with a similar weight of $\exp\{-S[U]\}$.

To derive the method in more detail we define an ensemble of configurations as an infinite collection of configuration states of the field U, with a density $W[U]$ defined on the measure dU [15]. Furthermore, the canonical ensemble (also referred to as the equilibrium ensemble, not related to the grandcanonincal or the microcanonical ensemble from statistical physics) is required to have a density W_c proportional to the Boltzman term:

$$W_c[U] \propto e^{-S[U]} \tag{5.2}$$

In numerical simulations we generate a finite number of configurations $\{[U_n],\ n = 1, 2, \ldots, N\}$ such that the samples approximate in their distribution the distribution of the canonical ensemble. By noting that the

ensemble average of a given operator $\overline{\overline{\mathcal{O}}}$ is equivalent to the expectation value of the operator $\langle\mathcal{O}\rangle$, and further noting that the sample average defined as:

$$\overline{\mathcal{O}} = \frac{1}{N}\sum_{n=1}^{N}\mathcal{O}[U_n] \tag{5.3}$$

is an estimator of the ensemble average, we may approximate the expectation value by computing a finite number of states.

The question remains however; how to generate a sequence of valid configurations $[U_n]$ such that the desired properties hold? What is used in practice is an updating procedure, defined as an algorithm that uses a currently existing configuration state $[U_n]$ to generate a new state $[U_{n+1}]$. Such an updating step is a stochastic random process in which each transition from state $[U] \to [U']$ is accompanied with a corresponding transition probability $P([U'] \leftarrow [U])$.[2] As a matter of notation, the updating of a single link is usually referred to as a step, and updating the entire lattice is referred to as a sweep. This is due to the fact that the majority of updating algorithms update link by link. In practice such systems are usually parallelized, on either the CPU, or more recently the GPU[21], allowing for concurrent updating of multiple links on the lattice.

We may also examine the effect of the transition probability on the ensemble of configurations defined earlier by noting that the ensemble density is changed after an updating step according to

$$W'[U'] = \sum_{[U]} P([U'] \leftarrow [U])W[U] \equiv \int dU P([U'] \leftarrow [U])W[U] \tag{5.4}$$

By considering the transition probability as a square matrix and the densities as vectors, we may rewrite this relation more succinctly in matrix notation as $W' = PW$. For the transition probability to be effective at updating some additional requirements must be placed upon it. Firstly, the transition probability must be normalized

$$\sum_{[U']} P([U'] \leftarrow [U]) \equiv \int dU' P([U'] \leftarrow [U])W[U] = 1 \tag{5.5}$$

Secondarily, strong ergodicity is required, defined as:

$$P([U'] \leftarrow [U]) > 0 \tag{5.6}$$

[2]Computers are generally not capable of producing purely random numbers. Instead pseudo-random numbers generators are used to simulate stochastic processes. This pseudo-random process produces a deterministic sequence of numbers based on a given seed. This deterministic property can be useful when attempting to replicate results.

for all pairs of configurations $(U,\ U')$. This allows every configuration to be reached from any other configuration with finite probability. Furthermore, it is assumed that a normalization condition is placed upon the density W,

$$\sum_{[U]} W[U] \equiv \int [dU] W[U] = 1 \tag{5.7}$$

Any stochastic process that satisfies the conditions specified in equations 5.4, 5.5, and 5.6 is referred to as a Markov process. The sequence of configurations is defined to be a Markov chain, and the entire process Markov Chain Monte Carlo (MCMC).

Now considering a "reasonable" (defined below) initial ensemble of configurations with corresponding density W_0, a condition must be placed on the updating process, such that through repeated applications of the updating procedure the resulting ensemble must be canonical ensemble

$$\lim_{k\to\infty} P^k W_0 = W_c \tag{5.8}$$

As such one can begin the simulation from any reasonable initial configuration and obtain accurate results. Reasonable in this case requires that the initial ensemble density must have nonzero overlap with the canonical ensemble, however due to the requirement of strong ergodicity this is always true for all initial configurations. This property of the canonical ensemble results in it being a fixed point of the transition probability, in effect

$$PW_c = W_c \tag{5.9}$$

We further require that this fixed point is unique, otherwise the numerical simulation would produce non-unique results.

An alternative condition maybe placed upon the transition probability that is sufficient (but not necessary) to establish the result of equation 5.9, and is referred to as detailed balance

$$P([U'] \leftarrow [U]) W_c[U] = P([U] \leftarrow [U']) W_c[U'] \tag{5.10}$$

Noting that this (eq. 5.10) in conjunction with equation 5.4 imply that

$$\sum_{[U]} P([U'] \leftarrow [U]) W_c[U] = \sum_{[U]} P([U] \leftarrow [U']) W_c[U'] = W_c[U'] \tag{5.11}$$

Which is equivalent to equation 5.9. The requirement given by equation 5.5 is also satisfied by detailed balance and may be proved through use of the theorem of Perron.

As discussed in the previous section, the operators that describe the glueball states consist of closed loops on the lattice, with periodic boundary conditions in place. Every spatial lattice point is considered as a starting point of such a loop, the sum over all of these loops in computed and divided by the total number of lattice points to obtain a single measure of the operator on the configuration. However, to determine the masses of glueballs we are also required to measure the 2-point correlation functions between various glueball states. The correlation between two lattice operators, A and B is defined as:

$$(AB) \equiv \langle \hat{A}\hat{B} \rangle = \frac{1}{Z} \int \mathcal{D}U \hat{A}[U] \hat{B}[U] e^{-S[U]} \tag{5.12}$$

in which an operator with a caret is defined to be the vacuum subtracted operator, $\hat{O} = O - \langle O \rangle$. By exploiting the linear properties of integrals, we may note that

$$\begin{aligned} \langle \hat{A}\hat{B} \rangle &= \langle (A - \langle A \rangle)(B - \langle B \rangle) \rangle \\ &= \langle AB \rangle - \langle A\langle B \rangle \rangle - \langle B\langle A \rangle \rangle + \langle \langle A \rangle \langle B \rangle \rangle = \langle AB \rangle - \langle A \rangle \langle B \rangle \end{aligned} \tag{5.13}$$

Which is the alternative, and often more conventional definition of the correlation. The masses of glueballs are determined by examining correlations between glueball states on different time slices. If we define one of the glueball states as a function of the time coordinate on the lattice as

$$\mathcal{O}_t = \frac{1}{V} \sum_{\mathbf{x}} \mathcal{O}_{\mathbf{x}t} \tag{5.14}$$

in which V is the number of spatial lattice points and $O_{\mathbf{x}t}$ are the Wilson loop operators described in the previous section with starting location $(\mathbf{x}, t)$. Then the correlation between various time states of the operators has, as shown in chapter 4, asymptotic behaviour of

$$\langle \hat{\mathcal{O}}_{t+t_0} \hat{\mathcal{O}}_{t_0} \rangle \simeq C(e^{-mt} + e^{-m(T-t)}) \tag{5.15}$$

In which C is a constant, T is the time dimension of the lattice, and m is the desired mass. The asymptotic relation holds only in the case of $t, T \to \infty$, implying that larger lattices give more accurate results. By taking the value of correlations for all values of t on the lattice and then fitting the curve a value of m may be determined.

It must be noted that the introduction of a finite number of lattice points will also affect the mass spectrum. It has been shown repeatedly that if a quantum field is enclosed in a box of a certain size L that mass spectrum will

obtain a dependence upon L, this is also true on the lattice [22]. These effects are referred to as finite size effects and must be taken into account when attempting to extrapolate results determined on the lattice to the continuum with infinite volume. Usually this is completed by measuring the same values on lattices of multiple sizes and then determining the change due to the varied volume.

The accuracy of the measured operators must still be considered. If the operators, $\mathcal{O}$, measured on the lattices configurations were statistically independent the sample average would simply be normally distributed around a mean of the ensemble average $\overline{\overline{\mathcal{O}}}$ with a variance of

$$\sigma^2_{\overline{\mathcal{O}}} = \frac{1}{N-1}(\overline{\mathcal{O}^2} - \overline{\mathcal{O}}^2) = \frac{1}{N-1}\overline{(\mathcal{O} - \overline{\mathcal{O}})^2} \tag{5.16}$$

This result is easily established by the central limit theorem. In this case the value of the average operator could simply be reported as $\overline{\overline{\mathcal{O}}} = \overline{\mathcal{O}} \pm \sigma_{\overline{\mathcal{O}}}$. Unfortunately, the updating procedure produces states that are dependent upon and often similar to each other. As such a more sophisticated measure of variance is required. The autocorrelation is defined to be the correlation between various configurations of the generated sequence. For values that are computed by means of averages on the lattice it is defined to be

$$\begin{aligned}(\mathcal{O}_n\mathcal{O}_{n+\tau}) &\equiv \langle \mathcal{O}_n\mathcal{O}_{n+\tau}\rangle - \langle \mathcal{O}_n\rangle\langle \mathcal{O}_{n+\tau}\rangle \\ &= \langle \mathcal{O}_n\mathcal{O}_{n+\tau}\rangle - \langle \mathcal{O}\rangle^2 = \langle (\mathcal{O}_n - \overline{\mathcal{O}})(\mathcal{O}_{n+\tau} - \overline{\mathcal{O}})\rangle\end{aligned} \tag{5.17}$$

Note that in this case the coordinate τ does not refer to a time coordinate on the lattice, but instead to the τth lattice configuration. The true variance of $\overline{\mathcal{O}}$ may be computed with respect to the autocorrelation to be

$$\begin{aligned}\sigma^2_{\overline{\mathcal{O}}} = \left\langle \left[\frac{1}{N}\sum_{n=1}^{N}(\mathcal{O}_n - \langle\mathcal{O}\rangle)\right]^2 \right\rangle &= \sum_{\tau=-N}^{N}\frac{N-|\tau|}{N^2}(\mathcal{O}_n\mathcal{O}_{n+\tau}) \\ &\xrightarrow{N\to\infty} (\mathcal{O}\mathcal{O})\frac{2\tau_{int,\mathcal{O}}}{N} \simeq (\overline{\mathcal{O}^2} - \overline{\mathcal{O}}^2)\frac{2\tau_{int,\mathcal{O}}}{N}\end{aligned} \tag{5.18}$$

In limit of $N \to \infty$ we have introduced the term $(\mathcal{O}\mathcal{O})$ which is the true correlation which is only available in this limit. The approximation in the final term is used in practice.

The integrated autocorrelation time $\tau_{int,\mathcal{O}}$ is given by:

$$\tau_{int,\mathcal{O}} \equiv \frac{1}{2}\sum_{\tau=-\infty}^{+\infty}\frac{(\mathcal{O}_n\mathcal{O}_{n+\tau})}{(\mathcal{O}\mathcal{O})} \tag{5.19}$$

As a direct result of the autocorrelation between various configuration states the number of statistically independent measurements is reduced to $N/2\tau_{int,\mathcal{O}}$. To ensure accurate results, when generating configurations at least $2\tau_{int,\mathcal{O}}$ updating sweeps are completed between measurements of the operators. This allows for the definition of variance given by equation 5.16 to be used in the measurement of operators.

In order to reduce the variance further a number of statistical techniques were implemented when measuring on the lattice. These techniques include, overrelaxation when generating new configurations to reduce auto-correlation, the multihit algorithm to reduce the variance in the measurement of operators, the multilevel algorithm to reduce the variance in correlations between operators, the variational method to produce composite operators that more accurately reflect the glueball states, and jacknife analysis for more reliable estimates of the error of measured quantities. All of these methods are discussed in more detail below.

5.1 Pseudo-Heatbath

A natural choice for the canonical distribution of configuration states, that was discussed in the previous section, would be to choose a transition probability matrix that is independent of the initial states,

$$P([U'] \leftarrow [U]) = W_c[U'] = Z^{-1} e^{-S[U']} \tag{5.20}$$

It can easily be shown that this transition probability satisifies the required properties, including strong ergodicity and detailed balance. The direct implementation of such transition probability is in practice impossible due to the large number of potential configurations. A heatbath algorithm, applies 5.20 locally; updating a single link while keeping all other field variables constant. The name "heatbath" is in reference to thermodynamics thought experiments, as the process of updating is similar to bringing a single link in contact with an infinite heatbath.

To define the transition probability for heatbath algorithms in more detail we define U_x to be the single link at space-time position x that will be updated. We further define $\check{U}_x$ as the set of all field variables, excluding the link U_x, that will remain fixed during the updating procedure. We may then define the conditional probability distribution of U_x in the canonical ensemble $W_c(U_x|\check{U}_x)$ as

$$W_c[U] \equiv W_c(U_x, \check{U}_x) \equiv W_c(U_x|\check{U}_x)\check{W}_c(\check{U}_x) \tag{5.21}$$

The conditional transition probability function for the update is similarly expressed as $P_x(U'_x \leftarrow U_x|\check{U}_x)$, with the total transition matrix defined as

$$P_x([U'] \leftarrow [U]) = P_x(U'_x \leftarrow U_x|\check{U}_x)\delta(\check{U}'_x - \check{U}_x) \tag{5.22}$$

We assume that the probability matrix satisfies the conditions of 5.4 and 5.6. With reference to 5.6 another sufficient (but not necessary) condition that satisfies this requirement is local detailed balance:

$$P_x(U'_x \leftarrow U_x|\check{U}_x)W_c(U_x|\check{U}_x) = P_x(U_x \leftarrow U'_x|\check{U}_x)W_c(U'_x|\check{U}_x) \tag{5.23}$$

Because of the fact that the local updating step only acts on a single link the process is naturally not ergodic. An alternative condition is therefore is therefore required, local ergodicity defined as

$$P_x(U'_x \leftarrow U_x|\check{U}_x) > 0 \tag{5.24}$$

Ergodicity maybe achieved on the entire system by performing a "sweep", or locally updating all of the links on the lattice, resulting in a total probability matrix

$$P([U'] \leftarrow [U]) = \prod_x P_x([U'] \leftarrow [U]) \tag{5.25}$$

The equations 5.21 - 5.25 are generic and describe any local updating procedure on the lattice, including, for example, the metropolis algorithm. The local heat bath algorithm corresponds specifically to the choice of conditional transition probability matrix of

$$P_x(U'_x \leftarrow U_x|\check{U}_x) = W_c(U'_x|\check{U}_x) \tag{5.26}$$

We may note that this is the local equivalent to equation 5.20. As such the task required of any heatbath algorithm is to produce the conditional distribution $W_c(U'_x|\check{U}_x)$ numerically. We may note specifically that if the integral of the distribution is known:

$$\mathrm{d}E_{\check{U}_x}(U_x) \equiv W_c(U'_x|\check{U}_x)\mathrm{d}U_x \tag{5.27}$$

in which $\mathrm{d}E_{\check{U}_x}(U_x)$ is the measure of this known integral, then due to the translational invariance of the measure, a random number $r \in [0, 1]$ may be used to generate a distribution U'_x by

$$U'_x = E^{-1}_{\check{U}_x}\left[E_{\check{U}_x}(a) + r[E_{\check{U}_x}(b) - E_{\check{U}_x}(a)]\right] \tag{5.28}$$

in which $[a, b]$ is the range that the field variables can take and $E^{-1}_{\check{U}_x}$ is the inverse of the function $E_{\check{U}_x}$.

Unfortunately in practice the exact value of the integral and its inverse is often still too difficult to use or calculate. Accordingly, an approximation of the distribution $W_0(U'_x|\check{U}_x)$ with corresponding integral $E_{0\check{U}_x}(U_x)$ may be used instead. However, the introduction of the approximation requires an additional "accept-reject" step to correct the distribution. When a new configuration U'_x is obtained, a second random number $r' \in [0, 1]$ must be chosen. The new configuration U'_x is accepted only if

$$r' \leq \frac{W_c(U'_x|\check{U}_x)}{W_0(U'_x|\check{U}_x)} \qquad \min_{a \leq U_x \leq b} \frac{W_0(U_x|\check{U}_x)}{W_c(U_x|\check{U}_x)} \leq 1 \tag{5.29}$$

5.1.1 SU(2) Heatbath

In the case of SU(2) the heatbath algorithm was first developed by Creutz [23, 24]. We begin by noting that the action may be decomposed with respect to a single link U_x as

$$S[U] = -\frac{\beta}{N} \mathrm{Re}\,\mathrm{Tr}\{U_x S_x\} + \check{S}(\check{U}_x) \tag{5.30}$$

in which S_x is an $N \times N$ matrix which is the sum of the 6 "staples" of the link, and the check ˇ mark refers to variables independent of U_x. Each link is part of 6 plaquettes, see figure 5.1, if the link U_x is in the direction $\hat{\mu}$, denoted $U_{x;\hat{\mu}}$ the staple refers to a product

$$U_{x+\hat{\mu};\hat{\nu}} U_{x+\hat{\mu}+\hat{\nu};-\hat{\mu}} U_{x+\hat{\nu};-\hat{\nu}} \tag{5.31}$$

in which $\nu \neq \mu$ and ν can be negative as well as positive. As such the term S_x is given by

$$S_x = \sum_{\nu=-3,\pm\nu\neq\mu}^{3} U_{x+\hat{\mu};\hat{\nu}} U_{x+\hat{\mu}+\hat{\nu};-\hat{\mu}} U_{x+\hat{\nu};-\hat{\nu}} \tag{5.32}$$

In which ν ranges over the dimensions x, y, z, and t denoted by the index $0, 1, 2, 3$, respectively, see figure 5.1.

This decomposition of the action is possible in the case of the Wilson action as well as in many more complicated actions, provided that the action is build up linearly from loop variables. As we are in SU(2) all links may be

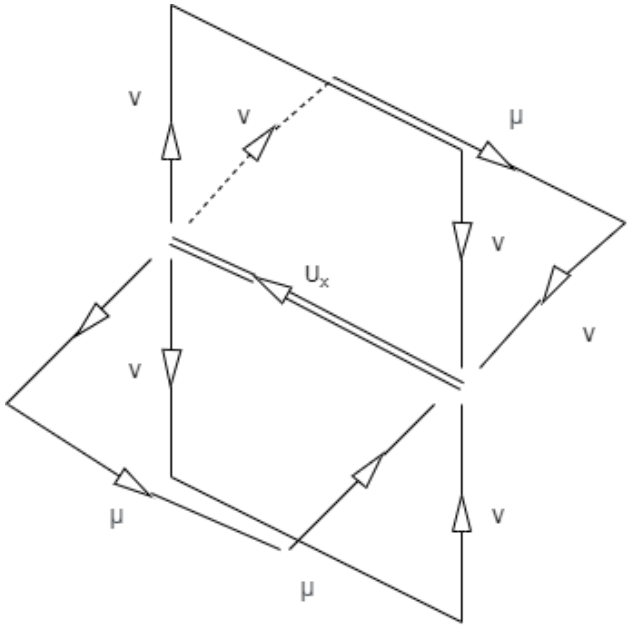

Figure 5.1: A link U_x with four of the staples shown. On a 4 dimensional space-time lattice each link has 6 total staples, only 4 are shown in this image. The arrows represent direction of traversal over the link in the multiplication step, using $U^{-1}_{x;\mu} = U_{x;-\mu}$

decomposed into sums over the identity and Pauli matrices, as such we define the link U_x and its adjoint $U^\dagger_x$ as

$$U_x \equiv a_{x0}\mathbf{1} + \sum_{r=1}^{3} i\sigma_r a_{xr} \quad U^\dagger_x = U^{-1}_x = a_{x0}\mathbf{1} - \sum_{r=1}^{3} i\sigma_r a_{xr} \tag{5.33}$$

where $\mathbf{1}$ is the 2×2 identity matrix and σ_r are the Pauli matrices. The unitarity of the link implies that

$$U^\dagger_x U_x = \sum_{r=0}^{4} a^2_{xr} = 1 \tag{5.34}$$

which implies that $a_{x0} = z_x(1 - |a_x|^2)^{1/2}$, in which $z_x = \pm 1$ and is a member of the Z_2 group and $|a_x|$ is defined as

$$|a_x| \equiv \left[\sum_{r=1}^{3} a^2_{xr}\right]^{1/2} \tag{5.35}$$

Similarly, the sum of the staples term S_x and its adjoint may similarly be represented as

$$S_x \equiv s_{x0}\mathbf{1} + \sum_{r=1}^{3} i\sigma_r s_{xr} \quad S_x^\dagger = s_{x0}\mathbf{1} - \sum_{r=1}^{3} i\sigma_r s_{xr} \tag{5.36}$$

This implies that given the product $S_x S_x^\dagger$, S_x^{-1} maybe obtained by

$$S_x S_x^\dagger = S_x^\dagger S_x = \sum_{r=0}^{3} s_{xr}^2, \quad S_x^{-1} = S_x^\dagger [\det\Big(S_x S_x^\dagger\Big)]^{1/2} = k^{-2} S_x^\dagger \tag{5.37}$$

in which

$$k^{-1} \equiv [\det\Big(S_x S_x^\dagger\Big)]^{1/4} = \left[\sum_{r=0}^{4} s_{xr}^2\right]^{1/2} = (\det(S_x))^{1/2} \tag{5.38}$$

From these relations we may note that the projection of S_x onto the $SU(2)$ group is given by $U_0 \equiv k S_x^{-1}$. Furthermore, letting the variables $a_r \equiv a_{xr}$, we note that on $SU(2)$ the invariant Haar measure, which is normalized to 1, is given by the equation

$$\begin{aligned} &\int \mathrm{d}U = \pi^{-2} \int \mathrm{d}^4 a \delta\left(\sum_{r=0}^{3} a_r^2 - 1\right) \\ &= \frac{1}{2\pi^2} \int \frac{\mathrm{d}a^4}{(1-|a|^2)^{1/2}} \left[\delta(a_0 - (1-|a|^2)^{1/2}) + \delta(a_0 + (1-|a|^2)^{1/2})\right] \theta(1-|a|^2) \end{aligned} \tag{5.39}$$

In which $\theta(x)$ is given by

$$\theta(x) = \begin{cases} 0 & x < 0 \\ 1 & x \geq 0 \end{cases} \tag{5.40}$$

The integral over the three dimensional vector $\vec{a} = \{a_1, a_2, a_3\}$ may equivalently be represented as

$$\begin{aligned} \frac{\mathrm{d}^3\vec{a}}{(1-|a|^2)^{1/2}} &= \mathrm{d}^3\vec{a} \exp\left\{\sum_{j=1}^{\infty} \frac{1}{2j} |a|^{2j}\right\} \\ &= \mathrm{d}|a| \frac{|a|^2}{(1-|a|^2)^{1/2}} \mathrm{d}^2\Omega_a = \mathrm{d}a_0 (1-a_0^2)^{1/2} \mathrm{d}^2\Omega_a \end{aligned} \tag{5.41}$$

In which $\mathbf{\Omega}_a$ is the solid angle with respect to the vector $\vec{a}$.

We may now use these equations to determine the conditional probability distribution of the link U_x, which may be written as

$$W_c(U_x|\check{U}_x)\mathrm{d}U_x \propto \exp\left\{\frac{\beta}{2}\,\mathrm{Tr}(U_x S_x)\right\}\mathrm{d}U_x = \exp\left\{\beta\sum_{r=0}^{3} a_{xr}s_{xr}\right\}\mathrm{d}U_x \quad (5.42)$$

noting that

$$U_x S_x = kU_x U_0^{-1} \equiv kU_{0x} \equiv k\left(a_0\mathbf{1} + \sum_{r=1}^{3} i\sigma_r a_r\right) \quad (5.43)$$

This variable U_{0x} is referred to as the transformed link. The transformed link allows for the simplification of the distribution. Due to the invariance of the Haar measure:

$$\int \mathrm{d}U_x W_c(U_x|\check{U}_x) = \int \mathrm{d}U_{0x} W_c(U_{0x}|\check{U}_{0x})$$

$$\rightarrow \int_{-1}^{1} \mathrm{d}a_0 (1-a_0^2)^{1/2} e^{\beta k a_0} \int \mathrm{d}^2\mathbf{\Omega}_a \quad (5.44)$$

This equation 5.44 is the distribution for the heatbath for single link on the lattice.

A single SU(2) link on the lattice can be updated by means of the heatbath algorithm through the following sequence:

1. First generate a random number a_0 from a uniform distribution with range $[-1, 1]$. This uniform distribution serves as the approximate distribution W_0 in equation 5.29.

2. Correct the distribution by accounting for the factor $(1-a_0^2)^{1/2}e^{\beta k a_0}$ by means of the accept-reject step discussed in equation 5.29. This accept-reject step may have to be repeated n times until acceptance is reached.

3. Generate the vector $\vec{a}$ randomly. The simplest manner is to use the fact that $\mathrm{d}\mathbf{\Omega}_a = \mathrm{d}\phi\mathrm{d}(\cos(\theta))$.

4. Finally, one may obtain the new link U_x' from the transformed link U_{0x} by means of $U_x' \equiv U_{0x}U_0$

More detailed implementations of the heatbath algorithm, including pseudo-code, may be found in other sources such as [15, 25].

5.1.2 The Pseudo-Heatbath for N>2

While the distribution for the one-link heatbath may be determined exactly for SU(2), difficulty arises with $SU(N)$ with $N > 2$. A heatbath algorithm for $SU(3)$ exists and was developed by Pietarinen [26]. For larger N algorithms have not been developed due to their complexity. Instead, for arbitrary N, Cabibbo and Marinari [27] developed an algorithm that applies the SU(2) heatbath algorithm on carefully chosen SU(2) subgroups of the SU(N) links. This algorithm is referred to as the pseudo-heatbath and is both efficient and effective at generating new configurations states even when N is large. Multiple improvements to the Cabibbo and Marinari psuedo-heatbath exist, such as increased computation efficiency [28], or the introduction of overrelaxation to decrease autocorrelation time [29] (see also section 5.2).

The algorithm first requires a selection of SU(2) subgroups. This subset of SU(2) subgroups, denoted by $\{SU(2)_k | k = 1, 2, \ldots, m\}$, must be chosen in such a way that no subset of $SU(N)$ is left invariant with respect to all selected subgroups. The collection proposed by Cabibbo and Marinari [27] is a collection of $m = N - 1$ subgroups, in which each subgroup is given by:

$$a_k = \begin{pmatrix} 1 & & & & & & \\ & \cdots & & & & & \\ & & 1 & & & & \\ & & & (\alpha_k) & & & \\ & & & & 1 & & \\ & & & & & \cdots & \\ & & & & & & 1 \end{pmatrix} \in SU(2)_k \tag{5.45}$$

in which α_k is a 2×2 matrix of the $SU(2)$ group located at the k and $k+1$th rows and columns.

An alternative collection also proposed by Cabibbo and Marinari [27] is to use the $m = (N(N-1)/2)$ subgroups whose significant values are placed at the intersections of the i and kth rows and collumns, in which i and k are not necessarily contiguous.

The updated link variable is subsequently determined by the repeated multiplication

$$U'_x = a_m a_{m-1} \cdots a_1 U_x \tag{5.46}$$

The definition may also be phrased recursively, defining $U_x^{(0)} \equiv U_x$ and $U^{(m)} \equiv U'_x$, we define each multiplicative step as

$$U_x^{(k)} = a_k U_x^{(k-1)} \tag{5.47}$$

Using this definition we may write that each of the subgroups a_k is drawn from the distribution

$$\mathrm{d}P_x(a_k) = \mathrm{d}^k a_k \exp\Big\{-S(a_k U_x^{(k-1)}, \check{U}_x)\Big\}\ Z_k^{-1}(U_x^{(k-1)}) \tag{5.48}$$

in which the measure $\mathrm{d}^k a_k$ is the Haar measure on the $SU(2)_k$ subgroup. The factor Z_k is given by

$$Z_k(U_x) \equiv \int_{SU(2)_k} \mathrm{d}a \exp\Big\{-S(aU_x, \check{U}_x)\Big\} = Z_k(bU_x) \tag{5.49}$$

where b is a constant. The validity of the final equality is due to the invariance of the Haar measure.

To show the usefullness of this approach we first show that the canonical distribution is left invariant under this series of steps. We shall show this inductively, first assuming that, following equation 5.20, $U_x^{(k-1)}$ has the following distribution

$$W_c(U_x^{(k-1)}, \check{U}_x)\mathrm{d}U_x^{(k-1)} = \exp\Big\{-S(U_x^{(k-1)}, \check{U}_x)\Big\}\ Z^{-1}\mathrm{d}U_x^{(k-1)} \tag{5.50}$$

Then the $U_x^{(k)} = aU_x^{(k-1)}$ must be distributed according to:

$$W_c(U_x^{(k)}, \check{U}_x)\mathrm{d}U_x^{(k)} =$$

$$\int_{SU(2)_k} \mathrm{d}^k a \frac{\exp\Big\{-S(U_x^{(k)}, \check{U}_x)\Big\} \exp\Big\{-S(a^{-1}U_x^{(k)}, \check{U}_x)\Big\}}{Z_k(a^{-1}U_x^{(k)})Z} \mathrm{d}(a^{-1}U_x^{(k)})$$

$$= \exp\Big\{-S(U_x^{(k)}, \check{U}_x)\Big\} Z^{-1}\mathrm{d}U_x^{(k)} \tag{5.51}$$

showing that if the initial $U_x^{(0)}$ has a canonical distribution, all subsequent $U_x^{(k)}$ will also have a canonical distribution, including $U_x^{(m)} = U'_x$. Finally the nature of the distribution needs to be determined. Using the definition of the decomposition of the action we note that:

$$S(a_k U_x, \check{U}_x) = -\frac{\beta}{N}\mathrm{Re}\,\mathrm{Tr}(a_k U_x S_x) + \check{S}(\check{U}_x)$$

$$= -\frac{\beta}{N}\mathrm{Re}\,\mathrm{Tr}(\alpha_k \rho_k) + \cdots \tag{5.52}$$

where the terms contained in the "$\cdots$" are all independent of α_k and the terms ρ_k represents the significant values of $U_x S_x$ that coincide with the positions of the significant values of a_k. Furthermore S_x is once again the

sum of the staples. As previously, by expanding the values of α_k and ρ_k as sums of Pauli matrices

$$\alpha_k \equiv \alpha_{k0}\mathbf{1} + \sum_{r=1}^{3} i\sigma_r \alpha_{kr} \quad \rho_k \equiv \rho_{k0}\mathbf{1} - \sum_{r=1}^{3} i\sigma_r \rho_{kr} \tag{5.53}$$

the term of the action dependent on α_k may be equivalently represented as

$$\frac{\beta}{N}\mathrm{Re}\,\mathrm{Tr}(\alpha_k \rho_k) = \frac{2\beta}{N}\sum_{r=0}^{3} \alpha_{kr}\mathrm{Re}(\rho_{kr}) \tag{5.54}$$

Therefore the probability distribution in equation 5.48 is given by

$$\mathrm{d}P(\alpha_k) \propto \mathrm{d}^4\alpha_k \delta\left(\sum_{r=0}^{3}\alpha_{kr} - 1\right)\exp\left\{\frac{2\beta}{N}\sum_{r=0}^{3}\alpha_{kr}\mathrm{Re}(\rho_{kr})\right\} \tag{5.55}$$

This distribution is equivalent to the distribution in equation 5.42 for the SU(2) heatbath. As such all values of α_k may be drawn using the same algorithm discussed in the previous section.

5.2 Overrelaxation

Overrelaxation algorithms for use in lattice field theory were first developed by Stephen Adler in the early 1980's [30]. These algorithms have consistently shown to decorrelate configurations significantly faster than pure heatbath methods. An overrelaxation algorithm transforms the configuration state of a single link by geometrically flipping its value around some global minimum. The overrelaxation algorithms are defined by a single parameter ω known as the overrelaxation parameter, which may take values in a range $\omega \in [0, 2]$. A parameter $\omega = 0$ results in no change to the system, while a parameter of $\omega = 1$ maps the configuration state directly to the global minimum, which is functionally identical to the heatbath algorithm. Pure overrelaxation schemes for updating links are not used commonly. In practice overrelaxation is used in conjunction with the heatbath algorithm to decorrelate configurations. In these cases a parameter of $\omega = 2$ is most commonly used and is referred to as the microcanonical limit. At this limit the ultraviolet modes of the system no longer evolve and the local action remains constant, but the individual links are changed. This allows for more rapid decorrelation of heatbath configurations.

The overrelaxation traditionally relied on actions that were multiquadratic, which by definition requires the action of a single link U_x to be able to be

decomposed into the form

$$S[U_x, \check{U}_x] = a(U_x - U_{0x})^2 + c \tag{5.56}$$

in which a, U_{0x}, and c are all functions of $\check{U}_x$. The overrelaxed update step is then given by

$$U'_x = \omega U_{0x} + (1-\omega)U_x + \omega(2-\omega)a^{-1/2}\eta \tag{5.57}$$

which may be shown to satisfy the condition of detailed balance, and therefore functions as an extension to the heatbath algorithm. In the equation above η is a real number drawn from unit Gaussian noise, and is optional. As previously mentioned, setting $\omega = 1$ returns the system to the heatbath algorithm in which U_{0x} is the new link parameter discussed in the previous section. Note that setting $\omega = 2$ the new action for a single link becomes

$$S[U_x, \check{U}_x] = a(-U_x + U_{0x})^2 + c \tag{5.58}$$

In effect the links have changed but the local action remains constant.

In the case of SU(2) a simple overrelaxation algorithm was developed by Brown and Woch [29] in which the relaxation parameter is set equal to $\omega = 2$. The authors noted that the following new update to a link U_x satisfies the requirements

$$U_x \to U'_x = V^\dagger U_x^\dagger V^\dagger \tag{5.59}$$

provided that that the gauge group element V is chosen to ensure that the action remains invariant. Let S_x be the sum of the staples of the link U_x (for a definition see the section 5.1). In the case of SU(2), the matrix S_x is proportional to the a group matrix. By defining $V = S_x/a$ in which $a = \sqrt{\det\{S_x\}}$ the matrix V is then normalized and unitary. As such the new action which is proportional to the term $\mathrm{tr}[U'_x S_x]$ may be shown to be invariant:

$$\mathrm{Tr}\Big[U'_x S_x\Big] = \mathrm{Tr}\Big[V^\dagger U_x^\dagger V^\dagger S_x\Big] = a\,\mathrm{Tr}\Big[V^\dagger U_x^\dagger\Big] = \mathrm{Tr}\Big[S_x^\dagger U_x^\dagger\Big] = \mathrm{Tr}[U S_x] \tag{5.60}$$

where the last step depends upon the reality of the trace of SU(2) matrices.

This algorithm may be implemented in $SU(N)$ by applying this microcanonical overrelaxation to all of the $SU(2)$ subgroups updated by the psuedo-heatbath algorithm.

Other overrelaxation algorithms exist that are specific to SU(3) such as the one by Pater [31], or one by Petronzio and Vicari [32]. Furthermore, several $SU(N)$ heatbath algorithms have been proposed such as the ones by Creutz [33] and one by de Forcrand and Jahn [34].

5.3 Multihit

The multihit algorithm was developed by Parisi, Petronzio, and Rapuanso in 1983 [35], in response to the often large statistical errors in lattice measurements. The fundamental question that was asked was whether it was possible, when measuring the expected value of an operator $\mathcal{A}$, to instead measure another operator $\mathcal{B}$, such that $\langle\mathcal{A}\rangle = \langle\mathcal{B}\rangle$, however such that the $\langle\mathcal{B}^2\rangle \ll \langle\mathcal{A}^2\rangle$. A measurement of this alternative operator would have a significantly smaller variance, and subsquently smaller statistical error in its measurement.

It was determined that in measuring the value of a single link U_x it was possible to replace the link with its multihit equivalent link $\overline{U}_x$ defined as by

$$\overline{U}_x = \frac{\int \mathcal{D}U \exp\{(\beta/N)\mathrm{Re}\,\mathrm{Tr}(U_x S_x)\}U_x}{\int \mathcal{D}U \exp\{(\beta/N)\mathrm{Re}\,\mathrm{Tr}(U_x S_x)\}} \tag{5.61}$$

In which S_x is once again the sum of the staples corresponding to the link U_x. The multihit link $\overline{U}_x$ is an improved estimator of the measured value. It may be noted that this equation is very similar in form to the single link integral with an external source which has been studied extensively, especially in the large N limit [36, 37, 38, 39, 40]. In the case of $SU(2)$ the value of $\overline{U}_x$ can be calculated in a close analytical form and may be shown to be

$$\overline{U}_x = \frac{I_2(2\beta K)}{I_1(2\beta K)} K S_x^{-1} \tag{5.62}$$

In which $K = |\det S_x|^{1/2}$ and I_2, I_1 are modified Bessel functions of the second and first kind, respectively. In the case that the links are in the adjoint, as opposed to the fundamental representation, alternative expressions exist [41]. In $SU(3)$ the integral may be computed numerically through a method developed by de Forcrand and Roiesnel [42], and requires the measure of a contour integral. For $SU(N)$ where $N > 3$ no convenient methods exists to determine a multihit link and instead the average must be computed be taking the average of M heatbath updates of the link. Note that the heatbath algorithm depends on the S_x of the link, all links will be drawn from the same statistical distribution.

Operators that consist of a number of links may have a subset of their links replaced by their corresponding multihit equivalents while ensuring that

$$\langle\mathcal{A}(U_1, U_2, \ldots U_n)\rangle = \langle\mathcal{A}(\overline{U}_1, \overline{U}_2, \ldots, \overline{U}_l, U_{l+1}, \ldots U_n)\rangle \tag{5.63}$$

However a condition must be placed that no two links that share a plaquette may both be replaced by their multihit counterpart. For the standard plaquette this implies that only a single link may be replaced by its multihit

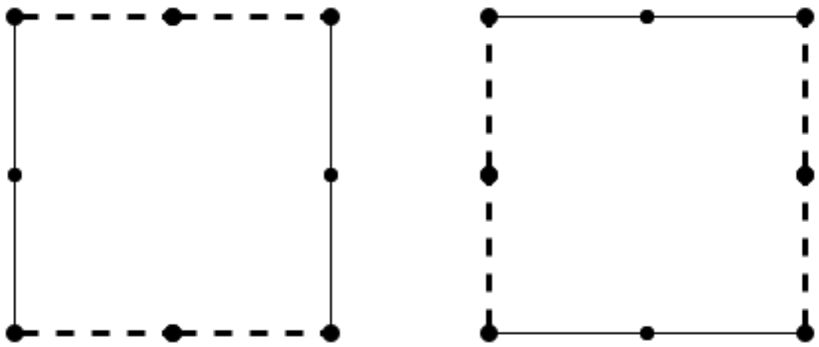

Figure 5.2: The various options for replacing links in the 2x2 Wilson loop with multihit links. Dashed lines represent links replaced by multihit links.

counterpart [43]. For 2×2 plaquettes a number of configuration states exist, see figure 5.2. For the measurement of a operator with multiple multihit configurations a single option may be chosen or an average options may be chosen. The average will most likely produce better results but requires more computational time.

5.4 Multilevel

The multilevel algorithm was first developed by Lüscher and Weisz [44] as a technique for variance reduction on the lattice. It was first tested on Polyakov loops (see of example [45]) but then expanded to two-point functions, for results see [46]. Similarly to the multi-hit algorithm it involves taking the average to reduce the variance, however the multilevel algorithm operates on time-slices and not individual operators.

The multilevel algorithm is based on locality. To describe this we follow an argument given by Meyer [13]. We denote a particular configuration with $\mathcal{C}$. On this configuration we define a number of mutually disjoint subsets denoted $\mathcal{A}, \mathcal{X}$, and $\mathcal{Y}$, with supports Ω_A, Ω_X and Ω_Y, respectively on the space-time manifold $\mathcal{M}$. We further suppose that for any continuous path $\gamma : I \to \mathcal{M}$ which joins Ω_x to Ω_Y the path passes through Ω_A.

Then if we have a theory with a probability distribution $p(\mathcal{C})$ it is defined to be local if functionals p_A and $\tilde{p}_A$ exist such that:

$$p(\mathcal{X}, \mathcal{Y}) = \sum_{\mathcal{A}} p(\mathcal{A}) p_A(\mathcal{X}) \tilde{p}_A(\mathcal{Y}) \tag{5.64}$$

Equivalently, this may be stated as the fact that $\mathcal{X}$ and $\mathcal{Y}$ only affect each other through $\mathcal{A}$. Meyer [13] points out that this condition is true for continuum

Euclidean field theories, provided that Lagrangian only contains a finite number of derivatives. Furthermore, this notion may be extended onto the lattice, however a suitable defintion of continuity must be defined. The Wilson action, used in this thesis, is local however the regions Ω_X and Ω_Y must be separated by more than one single lattice spacing.

The correlator of operators that are functionals of the subsets $\mathcal{X}$ and $\mathcal{Y}$, denoted by $\mathcal{O}_x$ and $\mathcal{O}_y$ respectively, may therefore be expressed as

$$\langle \mathcal{O}_x \mathcal{O}_y \rangle = \sum_{\mathcal{C}} \mathcal{O}_x \mathcal{O}_y p(\mathcal{C}) = \sum_{\mathcal{A}} \langle \mathcal{O}_x \rangle_A \langle \mathcal{O}_y \rangle_A \tag{5.65}$$

in which

$$\langle \mathcal{O}_x \rangle_A = \sum_{\mathcal{X}} p_A(\mathcal{X}) \mathcal{O}_x(\mathcal{X}) \tag{5.66}$$

$$\langle \mathcal{O}_y \rangle_A = \sum_{\mathcal{Y}} \tilde{p}_A(\mathcal{Y}) \mathcal{O}_y(\mathcal{Y}) \tag{5.67}$$

in essence, they are the averages of the operator $\mathcal{O}_i$ with $\mathcal{A}$ being fixed.

This decomposition may be applied in an iterative manner. By decomposing $\langle \mathcal{O}_i \rangle_A$ into the averages of smaller subspaces, the correlation function becomes recursively nested. For the three-levels equation 5.65 takes the form

$$\langle \mathcal{O}_x \mathcal{O}_y \rangle = \sum_{\mathcal{A}} \times \sum_{\mathcal{A}_1} p_A(\mathcal{A}_1) \sum_{\mathcal{A}_2} p_{A_1}(\mathcal{A}_2) \langle \mathcal{O}_x \rangle_{A_2} \times \tag{5.68}$$

$$\sum_{\tilde{\mathcal{A}}_1} \tilde{p}_A(\tilde{\mathcal{A}}_1) \sum_{\tilde{\mathcal{A}}_2} \tilde{p}_{\tilde{A}_1}(\tilde{\mathcal{A}}_2) \langle \mathcal{O}_y \rangle_{\tilde{\mathcal{A}}_2} \tag{5.69}$$

As such the multilevel algorithm involves the choosing of regions $\mathcal{A}$, fixing them in place and then updating and measuring on the regions $\mathcal{X}$ and $\mathcal{Y}$. In practice this is completed by choosing a set of time slices to be $\mathcal{A}$ and then to measure the operators in the regions of the lattice separated by these time slices. These measured time-slices are given a width of Δ and are updated a total of n times. If we update the boundary condition N_b times and measure the operators n times between each update we perform $N_{bc}n$ measurements. However due to the fact that the sums in equation 5.65 are factorized, this is equivalent to having performing $N_{bc}n^2$ measurements.

To obtain the result of $N_{bc}n^2$ some conditions must be met. First the measurements must be independent. Secondly, the fluctuation inside of Ω_x and Ω_y must have significantly more influence than the fluctuations on the

boundary Ω_a. And thirdly, the small volume and boundary conditions must not result in a phase transition. Provided that these conditions we are able to half the variance by doubling n, unlike ordinary variance reduction through Monte Carlo simulations which variance decreases as $\frac{1}{\sqrt{n}}$.

5.5 Variational Method

The variational method is used to find glueball state operators that better overlap with physical glueball states. It completes this task by constructing linear combinations of Wilson loop operators that measure the same glueball. The variational method may also be used to measure the excited states of glueballs, such as for example the 0^{++*} glueball. Consider a set of operators that all measure the same glueball state, represented by $\mathcal{O}_1, \mathcal{O}_2, \ldots, \mathcal{O}_n$. We then measure the cross correlations and store the values in a correlation matrix

$$C_{ij}(t) = \langle \hat{\mathcal{O}}_i(t)\hat{\mathcal{O}}_j(0)\rangle = \sum_{\tau=0}^{T-1} \langle \hat{\mathcal{O}}_i(t+\tau)\hat{\mathcal{O}}_j(\tau)\rangle \tag{5.70}$$

In which the $\hat{}$ symbol is used to represent a vacuum subtracted operator $\hat{\mathcal{O}} = \mathcal{O} - \langle \mathcal{O}\rangle$. For any value of $t \geq 0$ the general form of C_{ij} is given by [47]

$$C_{ij}(t) = \sum_{\alpha=1}^{\infty} v_i^{\alpha *} v_j^{\alpha} e^{-tE_\alpha} \tag{5.71}$$

in which

$$v_j^{\alpha} = \langle \alpha | \, \mathcal{O}_j(0) \, |0\rangle \quad \hat{H} \, |\alpha\rangle = E_\alpha \, |\alpha\rangle \tag{5.72}$$

Where $\hat{H}$ is the Hamiltonian of the theory, (see also section 4). Lüscher and Wolff [47] were able to prove that for every $t \geq 0$, and letting $\lambda_\alpha(t)$ be the eigenvalue of the correlation matrix $C(t)$ with ordering such that $\lambda_1 \geq \lambda_2 \geq \ldots \geq \lambda_r$, then for all $\alpha = 1, 2, \ldots, A$ we have

$$\lambda_\alpha(t) \underset{t\to\infty}{=} c_\alpha e^{-tE_\alpha} \left[1 + \mathcal{O}(e^{-t\Delta E_\alpha})\right] \tag{5.73}$$

In which $c_\alpha > 0$ is a constant and ΔE_α is the difference between E_α and another E_β. The mass, equivalent to the lowest lying energy state, could then be extracted by taking the ratio of the eigenvalues. Unfortunately, in this case the value of $C(t)$ at large t cannot be determined with a high degree of accuracy. This results in that the error term in equation 5.73 cannot be guaranteed to be negligible.

Instead of directly attempting to determine the eigenvalues Lüscher and Wolff proposed casting the problem into a generalized eigenvalue problem:

$$C_{ij}(t)\mathbf{v} = \lambda(t)C_{ij}(t_0)\mathbf{v} \tag{5.74}$$

in which $\mathbf{v}$ is the eigenvector, and $\lambda(t)$ is the corresponding eigenvalue, t_0 is fixed, small and usually taken to be 0. The authors similarly showed that in this case all λ still satisfy equation 5.73. However in this formulation the constant terms c_α are different and are expected to take a value around $c_\alpha \simeq e^{t_0 E_\alpha}$, while other terms are suppressed. As such this allows for accurate determination of the λ values even at large t. In the majority of cases the value of t used in 5.74 $t = 1$.

The generalized eigenvalue decomposition also allows the creation of a composite operator that more closely overlaps with the physical glueball states. By noting that the smallest eigenvalue, λ_0 corresponds to the lowest mass state, the corresponding eigenvector $\mathbf{v}^{(0)}$ may be used to construct a new operator $\mathcal{P} = \sum_i v_i^{(0)}\mathcal{O}_i$ such that the correlator

$$\langle\hat{\mathcal{P}}(t)\hat{\mathcal{P}}(0)\rangle \tag{5.75}$$

may be used to more accurately determine the mass of the glueball state. The second lowest eigenvalue may be used to determine the first exited state of the corresponding glueball. Subsequent eigenvalues may be used to approximate more excited states, however the signal to noise ratio rapidly deteriorates.

5.6 Jackknife

Jackknife analysis is a method of producing estimators for secondary quantities that more reliably give estimates of the error [15]. Secondary quantities are distinct from primary quantities which may be directly computed as averages, secondary quantities are functions of averages. The correlator is a common secondary quantity.

Jackknife resampling functions similarly to statistical bootstrapping techniques which are generally used for small sized samples. Jackknife resampling is more computationally efficient at large scales due to being a linear approximation of bootstrap.

Consider a set of measured values $A_1, A_2, \ldots, A_n$ and the primary quantity the average of this collection.

$$\overline{A} = \frac{1}{N}\sum_{n=1}^{N} A_n \tag{5.76}$$

Then a the secondary quantity y is best estimated by $\overline{y} = y(\overline{A})$. The jacknife average and variance of the sample gives a more stable estimator of $\overline{y}$. The jacknife average is computed by creating a set of averages of the total set of $\{A_n\}$ with a single element removed.

$$A_{(J)s} \equiv \frac{1}{N-1} \sum_{r \neq s} A_r \tag{5.77}$$

The values of the secondary quantity $y_{(J)s} = y(A_{(J)s})$ are referred to as jacknife estimators with a corresponding average

$$\overline{y_{(J)}} \equiv \frac{1}{N} \sum_{s=1}^{N} y_{(J)s} \tag{5.78}$$

with jacknife variance

$$\sigma^2_{(J)\overline{y}} \equiv \frac{N-1}{N} \sum_{s}^{N} \left(y_{(J)s} - \overline{y_{(J)}} \right)^2 \tag{5.79}$$

One may note that for primary quantities the jacknife variance and the simple variance are equivalent. However for secondary quantities the variance is often more reliable, the error may then be reported as $\overline{\overline{y}} = \overline{y} \pm \sigma_{(J)\overline{y}}$.

5.7 Code Architecture

The simulation code was first produced by Jelle Bor and Piter Annema. It was written in python 3.7 using of the numpy libraries for the required matrix manipulations. Due to problems of efficiency and paralellization the code was reimplemented into C and additional features were added by the author. For parallelization OpenMP[3] was used. Additional routines for matrix manipulations were adapted from the BLAS[4], LAPACK[5], and EISPACK[6] fortran routines.

The code architecture is as follows. The lattice itself is stored as an $R \times R \times R \times T \times 4 \times N^2$ complex double array. In which R and T are the number of spatial and temporal points along a particular axes, each point has 4 associated links, and each link is a complex $N \times N$ matrix. The lattice may be either randomly initialized, a hot start, or initialized with all matrices

[3] https://www.openmp.org/
[4] http://www.netlib.org/blas/
[5] http://www.netlib.org/lapack/
[6] http://www.netlib.org/eispack/

being the identity, a cold start. Furthermore when initializing the lattice a value for β must be given as well as a number of booleans that determine, what method for updating links is used (in this thesis only the heatbath), whether or not overrelaxation is used, and whether or not the code should be run in parallel. Furthermore additional parameters are used to determine the number of thermalization steps n_{therm}, the number of configurations that should be computed n_{conf} and the number of sweeps that should be completed between each configuration n_{corr}.

The lattice is then updated using the specified updating procedure. First the n_{therm} thermalization steps are completed, and then n_{conf} configurations are generated with n_{corr} sweeps in between. Each newly generated configuration is saved as a binary file to be read at later for analysis. Additionally, such a saved lattice may be read again at any point and more updates can be generated by using it as a seed. This allows the program to be cancelled and restarted from same point later.

Once the lattices have been generated the desired properties may be measured. First the operators to be measured must be specified by the user by means of a prototype Wilson loop. In this context prototype will mean any one of the spatial configurations of the Wilsoon loop. Secondarily the user must specify how the various spatial orientation must be summed together as this linear combination will determine which operator is measured (see section 4.3). Finally the desired T and C parity of the operator must be specified.

One the operators have been determined the measurement may begin. The user specifies which directory holds the saved lattices and over what range they wish to measure (i.e. from lattice 10 to 99). The method of analysis must be chosen, for example, measuring the correlator (with or without multihit), measuring the correlator using the multilevel algorithm, using the variational method, measuring the lattice spacing, etc. The operators are provided to the function as well as any other parameters that the measurement technique requires (e.g. n and Δ parameters in multilevel). The results are saved in a text file specified by the user.

Final processing of the measured data, including jackknife analysis, was completed using python. The numpy[7] library was used for matrix manipulation, scipy[8] was used for curve fitting, and matplotlib[9] was used for generating the graphs.

[7]https://numpy.org/
[8]https://www.scipy.org/
[9]https://matplotlib.org/

6 Results and Discussion

A number of simulations were run to compare various methods of error reduction. The focus of these simulations was on $SU(2)$, with variety of β values to allow for continuum extrapolation. For this purpose simulations were run on $12^3 \times 18$ lattices for β values of $1.8, 2.0$,and 2.2. The Psuedo-Heatbath method was used to generate individual configuration states with 10 sweeps and overrelaxation steps between each measurement. Furthermore all configurations were began from a cold initial state (ie. all links are set equal to identity matrices) and were thermalized with 300 sweeps, to allow the value of the average plaquette to settle.

6.1 Setting the scale

Before the values of operators can be measured we must first set the scale of the lattice. This allows us to convert glueball masses as measured on the lattice into physical units. We do this by determining the value of the lattice spacing a. The phsyical value of a is depended upon the β value of the lattice. We will set the scale by measuring the static quark potential and relating it to the hadronic scale parameter r_0.

r_0 is defined by the force between static quarks. It is given by:

$$r^2 \frac{dV(\vec{r})}{d\vec{r}}\bigg|_{r=r_0} = 1.65 \tag{6.1}$$

in which r is the distance between quarks and $V(r)$ is the static quark potential. The value of r_0 has been previously determined to be approximately $r_0 \approx 0.5$fm [48]. As such if we measure the static quark potential on the lattice we may use the hardronic scale parameter to determine a.

The expectation value of rectangular Wilson loops $W(\vec{r}, t)$, with lengths r and t on the lattice is well known to have the form

$$W(\vec{r}, t) = Z(\vec{r}) \exp\{-tV(\vec{r})\} + \cdots \tag{6.2}$$

In which $Z(\vec{r})$ is some function and the $\cdots$ represent excited-state contributions. We measured the value of the Wilson loops from $r = 2 - 10$ and with $t = 2 - 10$ and extracted $V(r)$ using a χ^2 least squares fitting technique.

The static quark potential was fitted with the model

$$V(\vec{r}) = V_0 + \sigma r + \frac{e_c}{r} \tag{6.3}$$

β	a/r_0	a(fm)
1.8	0.387(4)	0.194(2)
2.0	0.353(3)	0.176(2)
2.2	0.304(2)	0.152(1)

Table 6.1: The lattice spacing at different values of β determine by $r_0 \approx 0.5$

All three parameters V_0, σ and e_c were determined using another χ^2 least squares fitting method. Finally to determine the lattice spacing we make use of the relation (determined from equation 6.1):

$$\frac{a}{r_0} = \sqrt{\frac{\sigma}{1.65 + e_c}} \tag{6.4}$$

The values of the lattice spacing at the values of β measured may be found in table 6.1.

6.2 Glueball mass estimates

As noted in the previous section, once the configurations states have been generated, operators must be measured on the lattice to determine glueball masses. In this thesis we focus on the A_1^{++} glueball (0^{++} in the continuum) as it possess the lowest lying energy state. For multihit and multilevel two different operators for the $A_1^+ +$ operator were measured. The first was the plaquette, the $1x1$ planar rectangular Wilson loop. The A_1^{++} operator is the linear combination of the three spatial configurations of the plaquette, (xy-plane, xz-plane, yz-plane). The second operator measured is the $2x2$ rectangular spatial Wilson loop. Similarly to the plaquette the A_1^{++} operator is measured by the linear combination of the values of this loops 3 spatial configurations. With respect to the multihit, in the plaquette only one link may be replaced by its multihit counterpart, in the 2x2 loop 4 of the 8 links may be replaced, as shown in figure 5.2. The multilevel was run with the time slice thickness parameter Δ set equal to 4, and the number of sublattice updates n equal to 10.

The variational method generates an operator with greater overlap with a physical glueball state by a linear combination of other operators. As such when measuring the A_1^{++} state using the variational method we choose 3 operators to be combined: the plaquette (discussed above), the double plaquette, and the twisted plaquette (see figure 4.2, or B.4 for spatial orientations). Both the double and twisted plaquette are Wilson loops of length

6, the double plaquette has 6 spatial orientations, and the twisted plaquette has 4. While it is possible to combine the multihit and multilevel methods with the variational method, this was not completed by the author. As the variational method for n operators requires the computation of n^2 correlators, the addition of multihit and multilevel in the measurement of these operators was deemed too computationally expensive.

The mass was determined from the values of the correlators by means of the relation:

$$\langle \hat{\mathcal{O}}_{t+t_0} \hat{\mathcal{O}}_{t_0} \rangle \simeq C(e^{-mt} + e^{-m(T-t)}) \tag{6.5}$$

as discussed in the previous section. We may not that by taking the logarithm of the correlator and fitting a linear relationship for the first few values of t we may approximate the mass by the slope of the line. Furthermore when taking the logarithm, jacknife averages were used for more stable estimates of error.

It must be noted that in the following results there are some problem with the vacuum expectation value (VEV) subtraction. In the case of the multihit results, multihit techniques were not applied to the calculation of the VEV. In the case of the multilevel the VEV must be calculated on each individual subset of the lattice that is updated. In the present case the vacuum expectation value for the operator is calculated at the beginning of the measurement before the multilevel is applied. For the multihit, multilevel, and variational method this has resulted in the bottom of the parabola of the correlator measurement to be flattened. This further implies that the results for the glueball masses should be treated with scepticism. Despite this the results are still useful for determining the relative efficiency of the variance reduction algorithms. For an example of how this parabola should appear see image C.9 of some early results for the 2^{++} glueball. The 2^{++} glueball does not have the same quantum numbers as the vacuum and as such the vacuum expectation value does not have to be subtracted in this case. Note that in this case only 20 measurements were collected and due to noise some of the points are negative and not shown in the graph. Despite the lack of statistics it is still illustrative.

We first report the results for the multihit tests. The correlator for the plaquette may be seen in figure 6.1. The correlator value is displayed on a logarithmic axis and is the average of 840 measurements. It may be noted that the correlator takes the expected shape, that of a paraboloid with an expected minimum value around $t = 9$ (half of the maximum value of $T = 18$). The corresponding mass plot may be seen in figure 6.2, in which the first 3,

4, and 5 points have been used to determine the mass. Not that the mass is given by the negative of the slope. The value of the mass that is chosen is the one with the smallest percentage error.

In figure 6.3 we see the correlator measure of the 2x2 Wilson loop operator on the same $12^3 \times 18$ lattice at the same β value with 703 measurements. Its mass plot may be found in figure 6.4. We then show the results on the same lattice for the multihit + multilevel for the plaquette in figures 6.5 and 6.6 consisting of 824 measurements, and for the multihit + multilevel for the 2x2 Wilson loop in figures 6.7 and 6.8 consisting of 671 measurements.

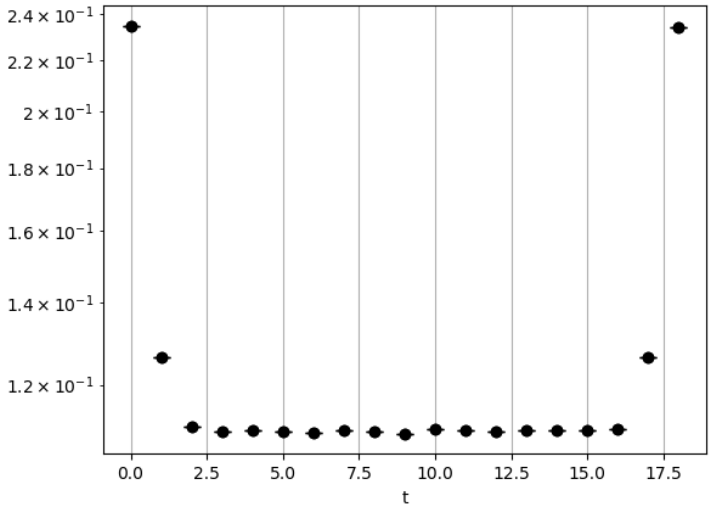

Figure 6.1: The correlation for the plaquette as a function of time, in SU(2) with lattice size 18×12^3, $\beta = 2.0$, 840 measurements, with multihit applied

Similar results for $\beta = 1.8, 2.2$ may be found in appendix C. What may be noted is that the values of the mass predicted by the 2x2 Wilson loops is much closer to the value of A_1^{++} operator found in previous studies such as 0.93 ± 0.3 [49] (at the continuum limit). This results may be explained by the fact that the plaquette has high ultra-violet divergences which could affect the measurement significantly. Despite this fact for both the plaquette as well as the 2x2 Wilson loop the multihit + multilevel combination resulted in smaller uncertainties than just the multihit.

The variational method was completed with the parameters specified above and the results for the correlator and the mass plot may be found in figures 6.9 and 6.10. The total number of measurements that was completed

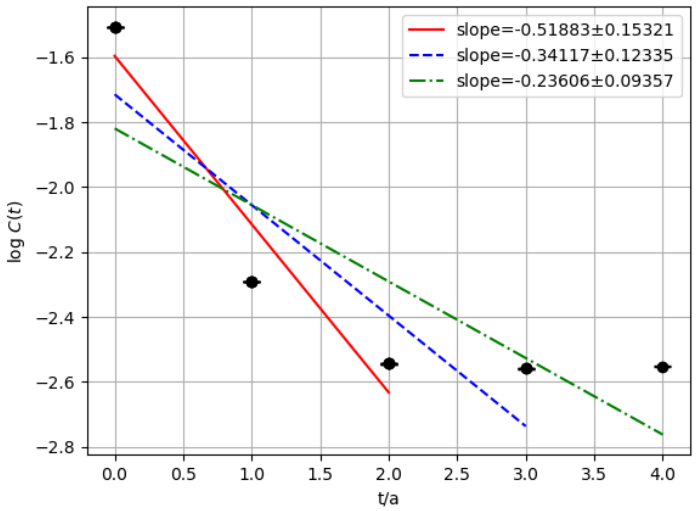

Figure 6.2: The mass plot for the A_1^{++} glueball as determined from the plaquette operator. Lattice size is $12^3 \times 18$, $\beta = 2.0$, 840 measurements, with mulithit. The three lines correspond to determining the mass from the first 3, 4, and 5 data points. mass $= -$slope

was 190. The reason for the significantly smaller sample size is due to the time complexity of the variational method. As the variational method with three operators, as in the present case, requires the computation of 9 correlators, the 190 measurements produced here is the equivalent of roughly 1700 ordinary correlator (without multihit or multilevel) measurements. The masses determined by the mass plot are accurate with respect to previous literature however the precision is lower than that of the mulithit + multilevel method, although this might simply be due to the limited statistics. As the variational method is more computationally expensive than the other methods the author recommends the use of those methods. This is further supported by the fact that the multilevel and multihit methods may be improved in precision by increasing the number of sublattice or one link updates. Every increase in sublattice or one link update scales the computational time linearly, ie if the number of updades is given by a, the computational time scales $\mathcal{O}(a)$. In contrast increasing the precision of the variational method requires an increase in the number of opertators n which scales computational time by $\mathcal{O}(n^2)$. Provided that the multihit + multilevel methods measure the correlators of operators that are not highly subject to ultraviolet divergences

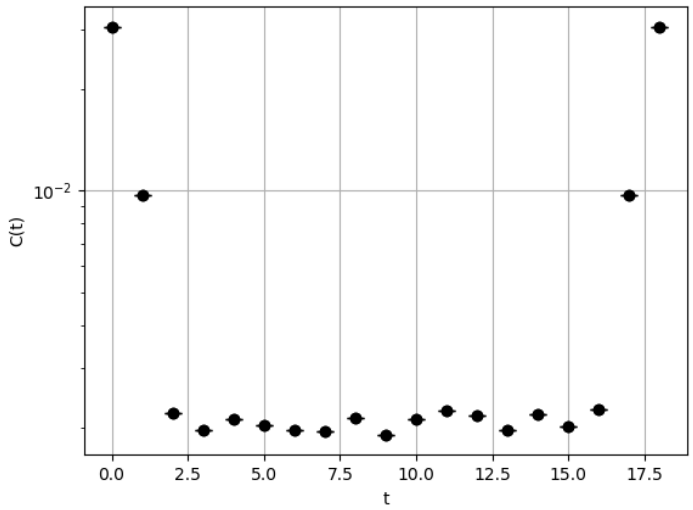

Figure 6.3: The correlation for the 2x2 Wilson loop as a function of time, in SU(2) with lattice size 18×12^3, $\beta = 2.0$, 703 measurements, with multihit applied

(such as the plaquette) their accuracy and precision are greater than the variational method, given a similar amount of computational time.

In large N measurements, such as those of $SU(8)$, for which this thesis is a prelimenary, the situation might be different. The multihit in $SU(N)$ with $N > 2$ requires a single link to be updated a number n_{hit} times to create a multihit link as an average. Furthermore, the multilevel requires the update of entire time slices of the lattice to produce averages. As both of these updating steps scale $\mathcal{O}(N^2)$. The variational method might be more computationally efficient at larger N values. Other techniques not discussed in this thesis, such as smearing and blocking of links, might also be more effective in large-N contexts.

A continuum extrapolation was completed to approximate the value of the A_1^{++} or equivalently the 0^{++} glueball at a lattice spacing of 0, using the multihit and multihit+multilevel results. The results for the multihit only may be found in figure 6.11,and for both multihit and multilevel in figure 6.12. Both graphs show the masses extrapolated to the continuum for the masses calculated with the first 3, 4, and 5 data points. The results for the glueball masses at the continuum may be found in table 6.2. May be seen from the figures the multihit method more accurately predicted the contiuum mass

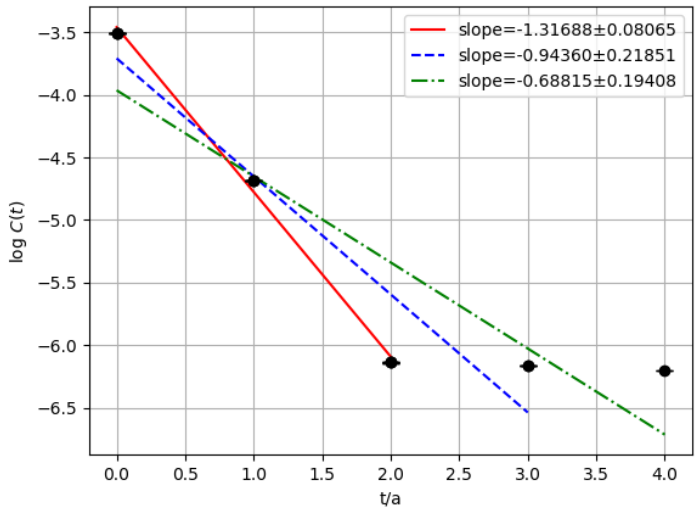

Figure 6.4: The mass plot for the A_1^{++} glueball as determined from the 2x2 Wilson loop operator. Lattice size is $12^3 \times 18$, $\beta = 2.0$, 703 measurements, with mulithit. The three lines correspond to determining the mass from the first 3, 4, and 5 data points. mass = −slope

of the 0^{++} glueball which has been previously estimated in the literature to be 0.93 ± 0.3 [49]. The multhit+multilevel method was more accurate in determining the glueball mass at any particular value of β, however the continuum extrapolation resulted in incorrect results. This inconsistency is most likely due to limited statistics. If glueball masses were determined using the multihit+multilevel method on more values of β with more measurements this error would most likely correct itself.

This thesis only performed measurements on $12^3 \times 18$ lattices. As such it is difficult to determine the scope of the finite size effects of the lattice on the measurements. Previous papers such as those by Langfeld [50] have shown that finite size effects are still present on lattices of 16^4, and therefore are most likely present in these results. However due to the relatively small statistics that were measured in this thesis it is possible that the remaining statistical noise is larger than the finite size effects. More measurements, including more measurements on lattices of different sizes, would have to be completed.

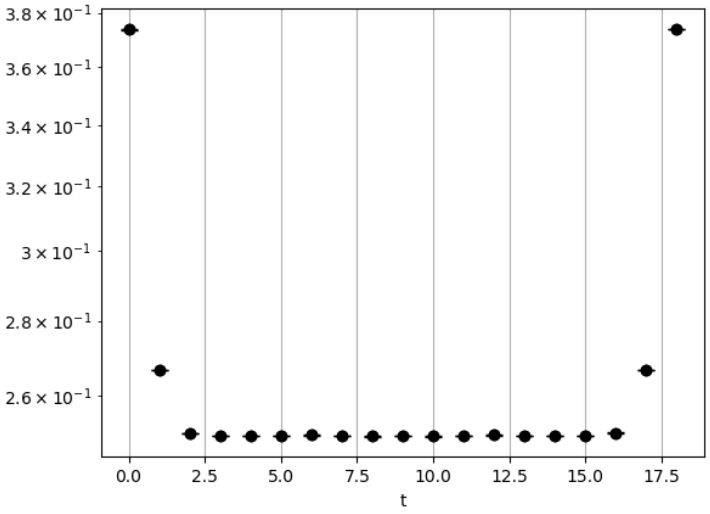

Figure 6.5: The correlation for the plaquette as a function of time, in SU(2) with lattice size 18×12^3, $\beta = 2.0$, 824 measurements with multihit and multilevel applied

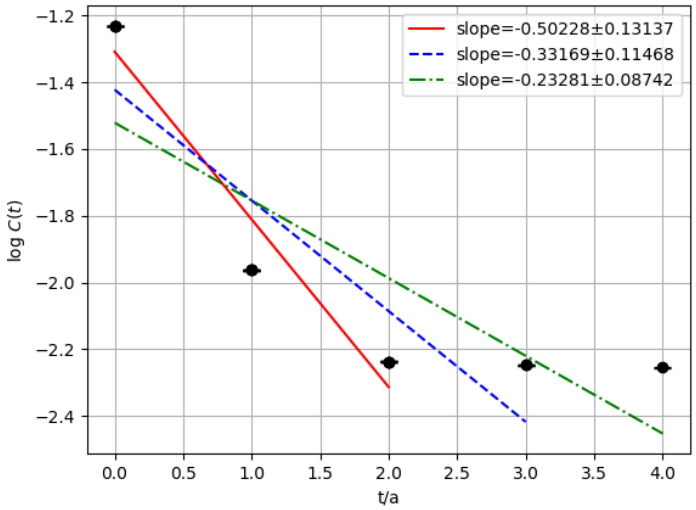

Figure 6.6: The mass plot for the A_1^{++} glueball as determined from the plaquette operator. Lattice size is $12^3 \times 18$, $\beta = 2.0$, 824 measurements, with mulithit and multilevel. The three lines correspond to determining the mass from the first 3, 4, and 5 data points. mass $= -$slope

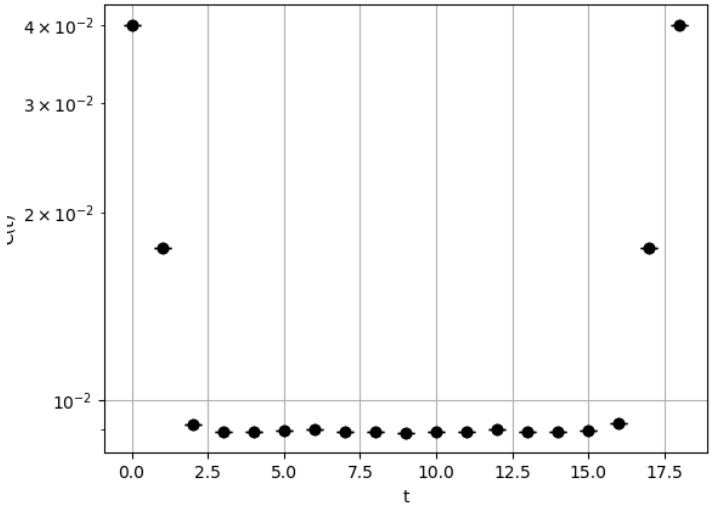

Figure 6.7: The correlation for the 2x2 Wilson loop as a function of time, in SU(2) with lattice size 18×12^3, $\beta = 2.0$, 671 measurements, with multihit and multilevel applied

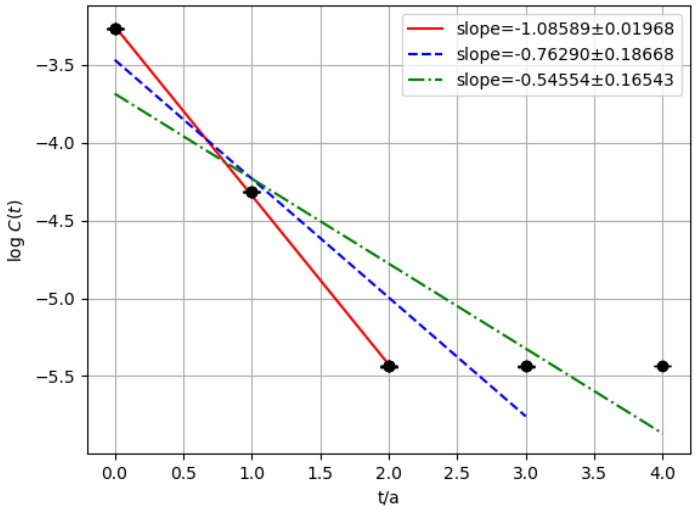

Figure 6.8: The mass plot for the A_1^{++} glueball as determined from the 2x2 Wilson loop operator. Lattice size is $12^3 \times 18$, $\beta = 2.0$, 671 measurements, with mulithit and multilevel. The three lines correspond to determining the mass from the first 3, 4, and 5 data points. mass = −slope

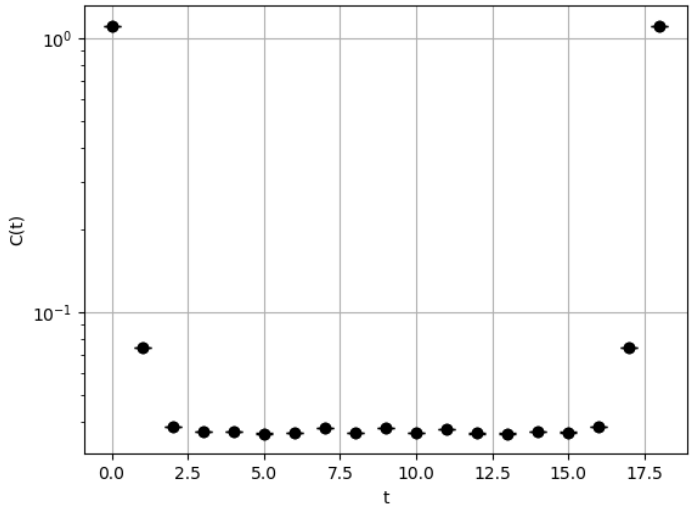

Figure 6.9: The correlation of the combined operator of the plaquette, double plaquette, and twisted plaquette (see figure 4.2) through the variational method as a function of time to measure the A_1^{++} glueball. Lattice size $12^3 \times 18$, with $\beta = 2.0$

Multihit 3 points	1.12
Multihit 4 points	1.26
Multihit 5 points	1.09
Multihit average	1.2 ± 0.1
Multihit + Multilevel 3 points	0.55
Multihit + Multilevel 4 points	0.78
Multihit + Multilevel 5 points	0.68
Multihit + Multilevel average	0.7 ± 0.2

Table 6.2: Value of the 0^{++} glueball mass at lattice spacing $a = 0$ determined via continuum extrapolation. Values determined from the first 3, 4, and 5 data points, and averaged.

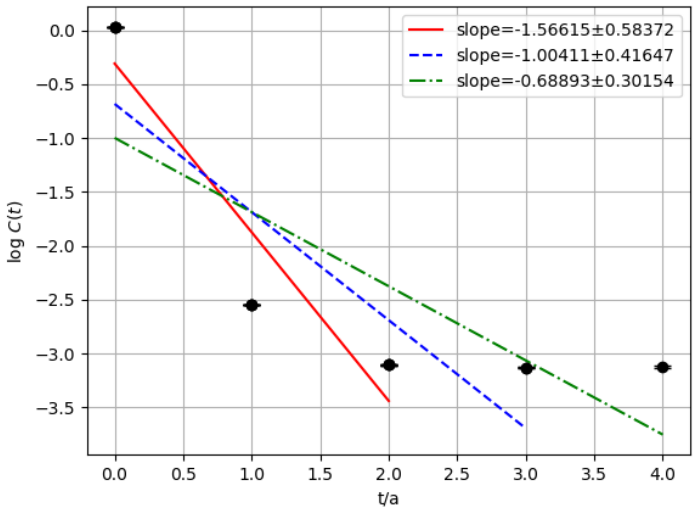

Figure 6.10: The mass plot for the A_1^{++} glueball as determined from the combined operator of the plaquette, double plaquette, and the twisted plaquette (see figure 4.2) as completed through the variational method. Lattice size is $12^3 \times 18$, $\beta = 2.0$. The three lines correspond to determining the mass from the first 3, 4, and 5 data points. mass = −slope

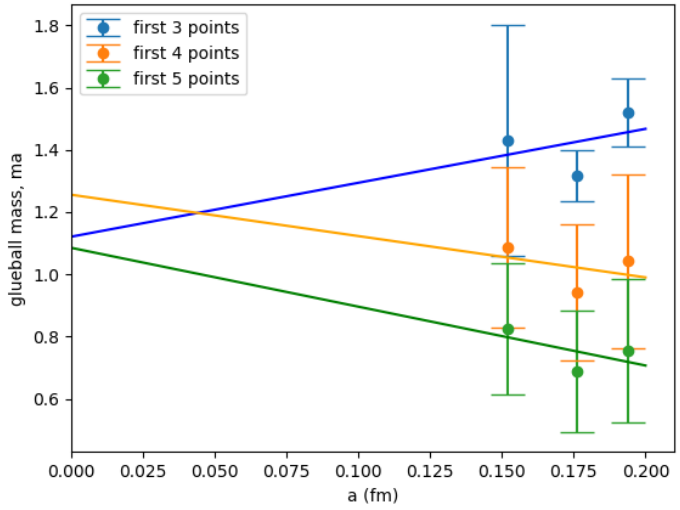

Figure 6.11: A continuum extrapolation for the glueball mass based on the the multihit results for beta 1.8, 2.0 and 2.2. The mass determined from the first three, four, and five data points in the their respective colors.

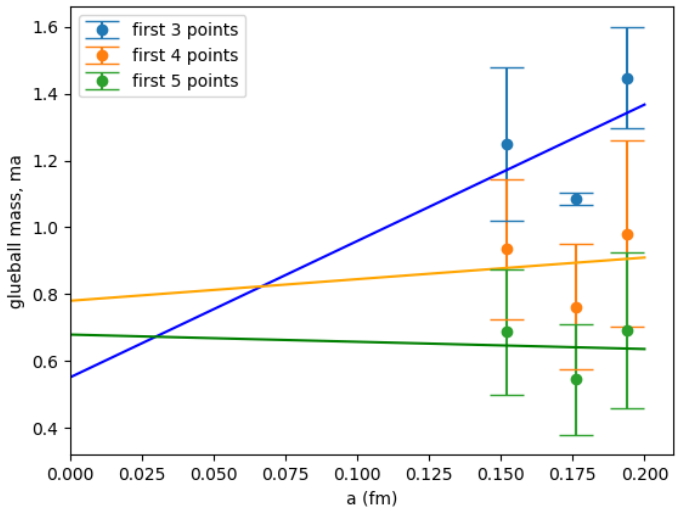

Figure 6.12: A continuum extrapolation for the glueball mass based on the the multihit+multilevel results for beta 1.8, 2.0 and 2.2. The mass determined from the first three, four, and five data points in the their respective colors.

7 Conclusion

Quantum chromodynamics as a theory to describe the strong force has existed since the early 1970's. The formulation of this theory on a Euclidean spacetime lattice, has allowed the study a host of properties predicted by QCD, including the hadron spectrum, decay constants, quark masses, form factors, and of course the glueball spectrum. Glueballs themselves being the resultant particles due to the self interactions of gluons. The rise of computing power, exemplified most prominently by Moore's law, but also by the continuous improvements in parallelization techniques, has meant that the study of lattice-QCD, which is uniquely representable in programmatic structures, has never been more accessible. The determination of glueball properties, including their masses, that are currently being completed on supercomputers are producing statistics previously unheard of. During this period of activity a number of new and old techniques for the generation of lattice states, and the reduction of error, have been brought to the forefront, some of which were discussed in this thesis.

We compared the effects of the multihit method, the multilevel method, and the variational method, for their ability to produce accurate glueball mass data. The multihit method involves replacing operators with alternative operators with identical mean but lower variance. The mulitilevel method similarly replaces correlators with alternative operators with similar means and lower variance. Finally the variational method produces a linear combination of operators with greater overlap with glueball base states. The variational method was traditionally used, often in conjunction with smearing and blocking of operators. However, in recent years the multihit and multilevel methods have grown in prominence.

Our results show that, in the particular cases tested, the multihit and multilevel methods in separate and in conjunction produce more accurate and more precise statistics for glueball masses than that of the variational method. We compared the multihit + multilevel in conjunction for both 1×1 plaquette, and 2×2 Wilson loops, against the variational method applied to three operators, the plaquette, double plaquette, and twisted plaquette. All tests were completed in $SU(2)$. The multihit and mulithit + multilevel techniques did not produce accurate results for the plaqutte. It has been observed in other papers [46], that the plaquette is susceptible to ultraviolet divergences, and therefore limits the effectivness of methods such as the multilevel. The use of the 2×2 Wilson loops gave more accurate results for both the multihit and the multihit+multilevel, with the latter being more

precise. The variational method did give accurate predictions for the lowest lying glueball mass but was less precise than other methods and required greater computing time.

Many possibilities were not tested in this thesis. The multihit technique is different in the special case of $SU(2)$ as it directly solvable. For other $SU(N)$ with $N > 2$, the multihit operator must instead be approximated by the average of m links generated through the psuedo-heatbath method. How the accuracy scales with m has not been determined. With regards to the multilevel, the algorithm efficacy is determined by two parameters. The number of sublattice updates, and the size of the time slice. The parameters were chosen to be 10 and 4 in this thesis by testing and comparing results and considering the available computational time. Previous works have had the number of sublattice updates as high as 25, requiring significantly more computing time for additional accuracy. For both the multihit and the multilevel accuracy may be improved by choosing alternative operators. In the present case we tested the plaquette and the 2×2 Wilson loop as both are simple operators with only 3 spatial orientations. The double plaquette of length 6 has 8 spatial orientations. While more complicated Wilson loops, even those of only length 8, may have well over 20 spatial orientations. For states such as the 0^{++} state all of these configurations must be measured. As such alternative choice of operator may be effective but could require significantly more computational time.

With regards to the variational method, many potential improvements exist. Firstly the introduction of more operators, unfortunately computational time scales quadratically with the number of operators. Secondarily would be the choice of operators with higher overlap with the physical ground state of the glueball. As previously mentioned this might be effective but must be compared to the increase in computational time resultant of more complicated operators. Furthermore, the variational method was not compared to the multihit and multilevel at larger N. The multihit and multilevel algorithms both require the updating of links to produce resutls. As the updating of links scales quadratically with N in a large N situation the variational method may become more computationally efficient compared. Finally the usage of the smearing and blocking of operators was note examined in this thesis. These technique replace links with the linear combination of itself and its neighbors, potentially offering greater improvement.

Besides serving as an evaluation of various statistical techniques to reduce the variance of operators measured on the lattice, this thesis also serves as a validation of lattice QCD simulation software written in part by the author.

In the long term the information gathered concerning the effectiveness of these various techniques will be used to produce large scale $SU(8)$ lattice simulations to measure the mass of the 0^{++} and 2^{++} glueballs. This research is being completed firstly, to test the accuracy of the large N solution of QCD given by Bochicchio[11]. As N increases the difference in the values of glueball properties between N and $N-1$ becomes smaller, $SU(8)$ is a reasonable approximation of the limit $N \to \infty$. Secondly the previous results for $SU(8)$ simulations produced by Lucini [12] and Meyer [13] contradict one another, this research will attempt to resolve this contradiction, and determine the true glueball spectrum for $SU(8)$.

8 Acknowledgements

The author would like to thank Prof. Elisabetta Pallante of the University of Groningen for her superivision during the course of the thesis. Furthermore, the author would like to thank Prof. Mauro Pappinutto and Prof. Marco Bochicchio from the Sapienza University of Rome, for allowing the author to use the Marconi supercomputer to collect some of the results in this paper.

References

[1] H. Fritzsch, M. Gell-Mann, and H. Leutwyler. "Advantages of the color octet gluon picture". In: *Physics Letters B* 47.4 (Nov. 1973), pp. 365–368. ISSN: 03702693. DOI: 10.1016/0370-2693(73)90625-4. URL: https://linkinghub.elsevier.com/retrieve/pii/0370269373906254.

[2] C. N. Yang and R. L. Mills. "Conservation of isotopic spin and isotopic gauge invariance". In: *Physical Review* 96.1 (1954), pp. 191–195. ISSN: 0031899X. DOI: 10.1103/PhysRev.96.191.

[3] David J. Gross and Frank Wilczek. "Ultraviolet Behavior of Non-Abelian Gauge Theories". In: *Phys. Rev. Lett.* 30 (26 June 1973), pp. 1343–1346. DOI: 10.1103/PhysRevLett.30.1343. URL: https://link.aps.org/doi/10.1103/PhysRevLett.30.1343.

[4] H. David Politzer. "Reliable Perturbative Results for Strong Interactions?" In: *Phys. Rev. Lett.* 30 (26 June 1973), pp. 1346–1349. DOI: 10.1103/PhysRevLett.30.1346. URL: https://link.aps.org/doi/10.1103/PhysRevLett.30.1346.

[5] Kenneth G. Wilson. "Confinement of quarks". In: *Phys. Rev. D* 10 (8 Oct. 1974), pp. 2445–2459. DOI: 10.1103/PhysRevD.10.2445. URL: https://link.aps.org/doi/10.1103/PhysRevD.10.2445.

[6] John B Kogut. "The lattice gauge theory approach to quantum chromodynamics". In: *Reviews of Modern Physics* 55.3 (1983), pp. 775–835. URL: https://journals.aps.org/rmp/pdf/10.1103/RevModPhys.55.775.

[7] Yigao Liang et al. "Lattice calculation of glueball matrix elements". In: *Nuclear Physics B* 307.C (1993), pp. 375–382. ISSN: 09205632. DOI: 10.1016/0920-5632(91)90906-U.

[8] Y. Chen et al. "Glueball spectrum and matrix elements on anisotropic lattices". In: *Physical Review D - Particles, Fields, Gravitation and Cosmology* 73.1 (2006), pp. 1–21. ISSN: 15502368. DOI: 10.1103/PhysRevD.73.014516.

[9] Long-Cheng Gui et al. "Study of the pseudoscalar glueball in J/ψ radiative decays". In: (2019), pp. 1–11. arXiv: 1906.03666. URL: http://arxiv.org/abs/1906.03666.

[10] Volker Crede. "The experimental status of glueballs". In: *AIP Conference Proceedings* 1182 (2009), pp. 471–474. ISSN: 0094243X. DOI: 10.1063/1.3293847. arXiv: arXiv:0812.0600v3.

[11] Marco Bochicchio. "An asymptotic solution of Large- N QCD, for the glueball and meson spectrum and the collinear S -matrix". In: *AIP Conference Proceedings* 1735.2015 (2016). ISSN: 15517616. DOI: 10.1063/1.4949387.

[12] B. Lucini. "The large N limit from the lattice". In: *Few-Body Systems* 36.1-4 (2005), pp. 161–166. ISSN: 01777963. DOI: 10.1007/s00601-004-0094-7. arXiv: 0410016 [hep-ph].

[13] Harvey B. Meyer. "Glueball Regge Trajectories". In: (2005). arXiv: 0508002 [hep-lat]. URL: http://arxiv.org/abs/hep-lat/0508002.

[14] Biagio Lucini, Antonio Rago, and Enrico Rinaldi. "Glueball masses in the large N limit". In: *Journal of High Energy Physics* 2010.8 (2010). ISSN: 11266708. DOI: 10.1007/JHEP08(2010)119. arXiv: arXiv:1007.3879v2.

[15] Istvan Montvay and Gernot Munster. *Quantum fields on a lattice*. Cambridge University Press, 1994. ISBN: 0 521 40432 0.

[16] Harald Fritzsch and Murray Gell–Mann. "Current Algebra: Quarks and What Else?" In: *Proceedings of the 16th International Conference On High-Energy Physics*. Vol. 2. 1972, pp. 135–165. DOI: 10.1142/9789812836854_0016. arXiv: 0208010 [hep-ph].

[17] B Berg and A. Billoire. "Glueball Spectroscopy in 4d SU(3) Lattice gauge theory (I)". In: *Nuclear Physics* 221.1 (1983), pp. 109–140.

[18] A. Ukawa and N. Kimura. "Energy-Momentum Dispersion of glueballs and the restoration of Lorentz invariance in lattice gauge theories". In: *Nuclear Physics* 205 (1982), pp. 637–647.

[19] S. L. Altmann and A. P. Cracknell. "Lattice Harmonics I. Cubic Groups". In: *Rev. Mod. Phys.* 37 (1 Jan. 1965), pp. 19–32. DOI: 10.1103/RevModPhys.37.19. URL: https://link.aps.org/doi/10.1103/RevModPhys.37.19.

[20] R. C. Johnson. "Angular Momentum on a Lattice". In: *Physics Letters B* 114.2 (1982), pp. 147–151.

[21] M. A. Clark et al. “Solving lattice QCD systems of equations using mixed precision solvers on GPUs”. In: *Computer Physics Communications* 181.9 (2010), pp. 1517–1528. ISSN: 00104655. DOI: 10.1016/j.cpc.2010.05.002. arXiv: arXiv:0911.3191v2.

[22] Gernot Munster. “The size of finite size effects in lattice gauge theories”. In: *Nuclear Physics* 249 (1985), pp. 659–671.

[23] Michael Creutz. “Confinement and the Critical Dimensionality of Space-Time”. In: *Phys. Rev. Lett.* 43 (8 Aug. 1979), pp. 553–556. DOI: 10.1103/PhysRevLett.43.553. URL: https://link.aps.org/doi/10.1103/PhysRevLett.43.553.

[24] Michael Creutz. “Monte Carlo study of quantized SU(2) gauge theory”. In: *Phys. Rev. D* 21 (8 Apr. 1980), pp. 2308–2315. DOI: 10.1103/PhysRevD.21.2308. URL: https://link.aps.org/doi/10.1103/PhysRevD.21.2308.

[25] Christof Gattringer and Christian B. Lang. *Quantum Chromodynamics on the Lattice*. Lecture Notes in Physics. Berlin, Heidelberg: Springer Berlin Heidelberg, 2010. ISBN: 978-3-642-01849-7. DOI: 10.1007/978-3-642-01850-3. arXiv: arXiv:1011.1669v3. URL: http://link.springer.com/10.1007/978-3-642-01850-3.

[26] E. Pietarinen. “String Tension in SU(3) Lattice Gauge Theory”. In: (Feb. 1981). Ed. by J. Julve and M. Ramón-Medrano, pp. 270–277. DOI: 10.1016/0550-3213(81)90565-4.

[27] Nicola Cabibbo and Enzo Marinari. “A new method for updating SU(N) matrices in computer simulations of gauge theories”. In: *Physics Letters B* 119.4-6 (1982), pp. 387–390. ISSN: 03702693. DOI: 10.1016/0370-2693(82)90696-7.

[28] A. D. Kennedy and B. J. Pendleton. “Improved Heatbath Method for Monte Carlo Calculations in Lattice Gauge Theories”. In: *Physics Letters B* 156.5 (1985), pp. 393–399.

[29] Frank R. Brown and Thomas J. Woch. “Overrelaxed heat-bath and Metropolis algorithms for accelerating pure gauge Monte Carlo calculations”. In: *Physical Review Letters* 58.23 (1987), pp. 2394–2396. ISSN: 00319007. DOI: 10.1103/PhysRevLett.58.2394.

[30] Stephen L. Adler. “Overrelaxation algorithms for lattice field theories”. In: *Physical Review D* 37.2 (1988), pp. 458–471. ISSN: 05562821. DOI: 10.1103/PhysRevD.37.458.

[31] R. Gupta et al. “Monte Carlo Renormalization Group for SU(3) Lattice Gauge Theory”. In: *Phys. Rev. Lett.* 53 (18 Oct. 1984), pp. 1721–1724. DOI: 10.1103/PhysRevLett.53.1721. URL: https://link.aps.org/doi/10.1103/PhysRevLett.53.1721.

[32] Roberto Petronzio and Ettore Vicari. “An overrelaxed Monte Carlo algorithm for SU (3) lattice gauge theories”. In: *Physics Letters B* 248.1-2 (1990), pp. 159–162. ISSN: 03702693. DOI: 10.1016/0370-2693(90)90032-2.

[33] Michael Creutz. “Overrelaxation and Monte Carlo simulation”. In: *Phys. Rev. D* 36 (2 July 1987), pp. 515–519. DOI: 10.1103/PhysRevD.36.515. URL: https://link.aps.org/doi/10.1103/PhysRevD.36.515.

[34] Philippe de Forcrand and Oliver Jahn. “Monte Carlo Overrelaxation for SU(N) Gauge Theories”. In: 2 (2005), pp. 67–73. DOI: 10.1007/3-540-28504-0_6. arXiv: 0503041v1 [arXiv:hep-lat].

[35] G. Parisi, R. Petronzio, and F. Rapuano. *A measurement of the string tension near the continuum limit*. 1983. DOI: 10.1016/0370-2693(83)90930-9.

[36] Richard C. Brower, Paolo Rossi, and Chung I. Tan. “Chiral chains for lattice quantum chromodynamics at N_c =\infty”. In: *Physics Review D* 23.4 (1981), pp. 942–952.

[37] E. Brezin and David J. Gross. “The external field problem in the large N limit of QCD”. In: *"Physics Letters, Section B: Nuclear, Elementary Particle and High-Energy Physics"* 97.1 (1980), pp. 120–124. ISSN: 03702693. DOI: 10.1016/0370-2693(80)90562-6.

[38] K. E. Eriksson, N. Svartholm, and B. S. Skagerstam. *On invariant group integrals in lattice QCD*. 1981. DOI: 10.1063/1.524760.

[39] Richard C. Brower and Michael Nauenberg. “Group integration for lattice gauge theory at large N and at small coupling”. In: *Nuclear Physics, Section B* 180.2 (1981), pp. 221–247. ISSN: 05503213. DOI: 10.1016/0550-3213(81)90416-8.

[40] Richard Brower, Paolo Rossi, and Chung I. Tan. “The external field problem for QCD”. In: *Nuclear Physics, Section B* 190.4 (1981), pp. 699–718. ISSN: 05503213. DOI: 10.1016/0550-3213(81)90046-8.

[41] C. Michael. “Adjoint sources in lattice gauge theory”. In: *Nuclear Physics, Section B* 259.1 (1985), pp. 58–76. ISSN: 05503213. DOI: 10.1016/0550-3213(85)90297-4.

[42] Ph de Forcrand and C. Roiesnel. “Refined methods for measuring large-distance correlations”. In: *Physics Letters B* 151.1 (1985), pp. 77–80. ISSN: 03702693. DOI: 10.1016/0370-2693(85)90826-3.

[43] H. Meyer-Ortmanns and I Montvay. “Monte Carlo study of glueball masses in SU(2)”. In: *Physics Letters B* 145.3-4 (1984), pp. 251–255. ISSN: 03702693. DOI: 10.1016/0370-2693(84)90349-6.

[44] Martin Lüscher and Peter Weisz. “Locality and exponential error reduction in numerical lattice gauge theory”. In: *Journal of High Energy Physics* 5.9 (2001), pp. 1–18. ISSN: 10298479. arXiv: 0108014v1 [arXiv:hep-lat].

[45] Nayasinganahalli Hari Dass and Pushan Majumdar. “High accuracy simulations of d=4 SU(3) qcd-string”. In: *Proceedings of Science* 20.3 (2005). ISSN: 18248039. arXiv: 0511055v1 [arXiv:hep-lat].

[46] Pushan Majumdar, Nilmani Mathur, and Sourav Mondal. “Noise reduction algorithm for glueball correlators”. In: *Physics Letters, Section B: Nuclear, Elementary Particle and High-Energy Physics* 736 (2014), pp. 415–420. ISSN: 03702693. DOI: 10.1016/j.physletb.2014.07.056. arXiv: arXiv:1403.2936v2.

[47] Martin Lüscher and Ulli Wolff. “How to calculate the elastic scattering matrix in two-dimensional quantum field theories by numerical simulation”. In: *Nuclear Physics, Section B* 339.1 (1990), pp. 222–252. ISSN: 05503213. DOI: 10.1016/0550-3213(90)90540-T.

[48] Colin J. Morningstar and Mike Peardon. “Efficient glueball simulations on anisotropic lattices”. In: *Physical Review D - Particles, Fields, Gravitation and Cosmology* 56.7 (1997), pp. 4043–4061. ISSN: 15502368. DOI: 10.1103/PhysRevD.56.4043.

[49] B. Berg. “Plaquette-plaquette correlations in the SU(2) lattice gauge theory”. In: *Physics Letters B* 97.3-4 (1980), pp. 401–404. ISSN: 03702693. DOI: 10.1016/0370-2693(80)90628-0.

[50] Kurt Langfeld. “Improved actions and asymptotic scaling in lattice Yang-Mills theory”. In: *Physical Review D - Particles, Fields, Gravitation and Cosmology* 76.9 (2007). ISSN: 15507998. DOI: 10.1103/PhysRevD.76.094502. arXiv: arXiv:0704.2635v2.

A Multiplicity of Irreducible Representations of the Cubic Group in Wilson Loop Operators up to Length 8

OP	d	A_1^{++}	A_2^{++}	E^{++}	T_1^{++}	T_2^{++}	A_1^{-+}	A_2^{-+}	E^{-+}	T_1^{-+}	T_2^{-+}
1	6	1	0	1	0	0	0	0	0	0	0
2	24	1	0	1	0	1	0	0	0	1	1
3	24	1	0	1	0	1	0	0	0	1	1
4	96	1	1	2	3	3	1	1	2	3	3
5	48	1	0	1	1	2	1	0	1	1	2
6	12	1	1	2	0	0	0	0	0	0	0
7	48	1	1	2	1	1	0	0	0	2	2
8	24	1	1	2	1	1	0	0	0	0	0
9	12	1	0	1	0	0	0	0	0	0	1
10	24	1	0	1	1	2	0	0	0	0	0
11	6	1	0	1	0	0	0	0	0	0	0
12	12	1	1	2	0	0	0	0	0	0	0
13	12	1	0	1	0	1	0	0	0	0	0
14	48	1	0	1	1	2	1	0	1	1	2
15	12	1	0	1	0	1	0	0	0	0	0
16	48	1	0	1	1	2	1	0	1	1	2
17	24	1	0	1	0	1	0	0	0	1	1
18	96	1	1	2	3	3	1	1	2	3	3

Table A.1: Multiplicities of irreducible representations of the cubic group O_h with $C = 1$ charge parity in the representation $\mathcal{M}$ or various operators of length 8. Number of the operator corresponds to figure 4.2

OP	d	A_1^{+-}	A_2^{+-}	E^{+-}	T_1^{+-}	T_2^{+-}	A_1^{--}	A_2^{--}	E^{--}	T_1^{--}	T_2^{--}
1	6	0	0	0	1	0	0	0	0	0	0
2	24	0	0	0	1	1	1	0	1	0	1
3	24	0	1	1	1	0	0	0	0	1	1
4	96	1	1	2	3	3	1	1	2	3	3
5	48	0	1	1	2	1	0	1	1	2	1
6	12	0	0	0	1	2	0	0	0	0	0
7	48	0	0	0	2	2	1	1	2	1	1
8	24	0	0	0	2	0	0	0	0	0	0
9	12	0	0	0	1	0	0	1	1	0	0
10	24	0	1	1	2	1	0	0	0	0	0
11	6	0	0	0	1	0	0	0	0	0	0
12	12	0	0	0	0	0	0	0	0	1	1
13	12	0	0	0	0	0	0	0	0	1	1
14	48	0	1	1	2	1	0	1	1	2	1
15	12	0	1	1	1	0	0	0	0	0	0
16	48	1	0	1	1	2	1	0	1	1	2
17	24	0	0	0	1	1	0	1	1	1	0
18	96	1	1	2	3	3	1	1	2	3	3

Table A.2: Multiplicities of irreducible representations of the cubic group O_h with $C = 1$ charge parity in the representation $\mathcal{M}$ or various operators of length 8. Number of the operator corresponds to figure 4.2

B Spatial Orientations and Constructable Wavefunctions of Additional Operators

Plaquette spatial orientations:

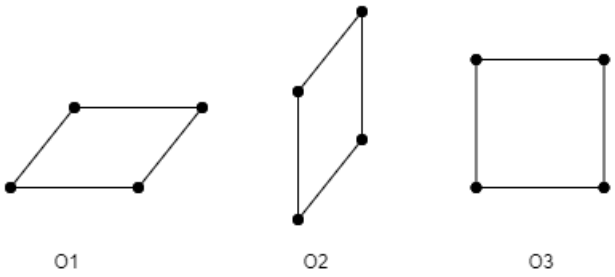

Figure B.1: The three spatial orientations of the plaquette.

Double plaqutte spatial orientations:

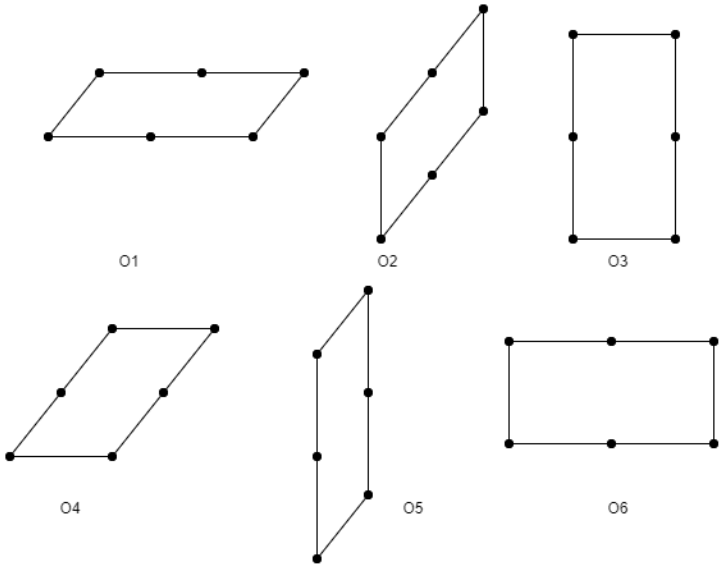

Figure B.2: The spatial orientations of the double plaquette.

Bent plaquettes:
Spatial orientation:

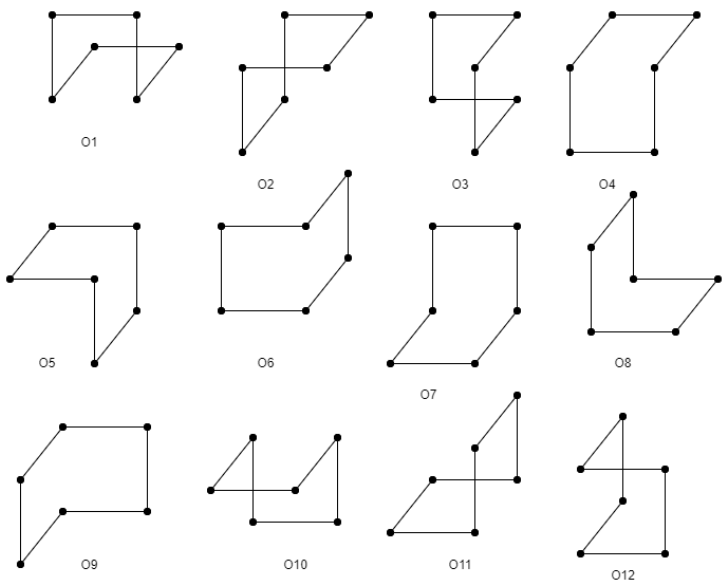

Figure B.3: The spatial orientations of the bent plaquette.

Wavefunction composition table:

	O_1	O_2	O_3	O_4	O_5	O_6	O_7	O_8	O_9	O_{10}	O_{11}	O_{12}
A_1^{++}, A_1^{--}	1	1	1	1	1	1	1	1	1	1	1	1
E^{++}, E^{--}	-1	1	0	-1	1	0	-1	1	0	-1	1	0
	-1	-1	2	-1	-1	2	-1	-1	2	-1	-1	2
T_1^{-+}, T_1^{+-}	-1	1	0	1	1	0	-1	-1	0	0	1	-1
	0	-1	1	0	1	1	0	-1	-1	0	1	-1
	1	0	-1	1	0	1	-1	0	-1	-1	0	1
T_2^{-+}, T_2^{+-}	1	1	0	-1	1	0	1	-1	0	-1	-1	0
	0	1	1	0	-1	1	0	1	-1	0	-1	-1
	1	0	1	1	0	-1	-1	0	1	-1	0	-1
T_2^{++}, T_2^{--}	0	0	1	0	0	-1	0	0	-1	0	0	1
	1	0	0	-1	0	0	-1	0	0	1	0	0
	0	1	0	0	-1	0	0	-1	0	0	1	0

Table B.1: Wavefunctions for various glueball states that may be constructed from the bent plaquette operator

Twisted Plaquette:
Spatial orientations:

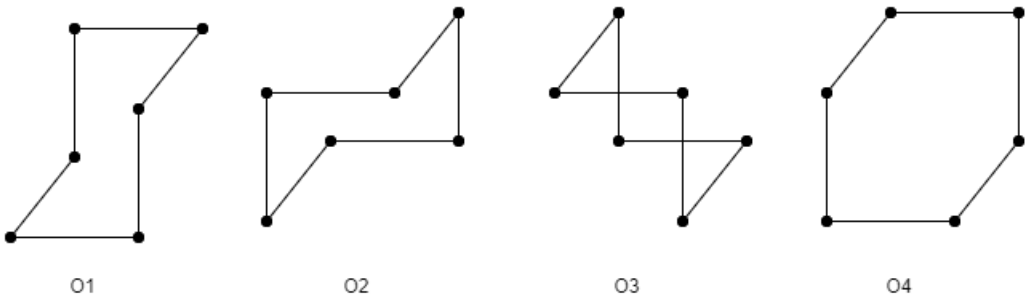

Figure B.4: The spatial orientations of the twisted plaquette.

Wavefunction composition table:

	O_1	O_2	O_3	O_4
A_1^{++}, A_2^{+-}	1	1	1	1
T_2^{++}, T_1^{+-}	1	-1	1	-1
	-1	1	1	-1
	1	1	-1	-1

Table B.2: Wavefunctions for various glueball states that may be constructed from the Twisted plaquette operator. For definition of O_i see figure X

C Glueball Correlators and Mass Estimates for $\beta = 1.8$ and 2.2

Multihit 2x2 loop $\beta = 1.8$

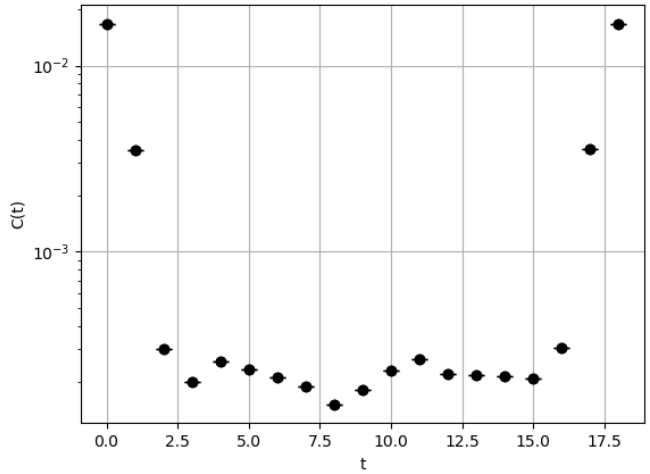

Figure C.1: The correlation for the 2x2 Wilson loop as a function of time, in SU(2) with lattice size 18×12^3, $\beta = 1.8$ with multihit applied

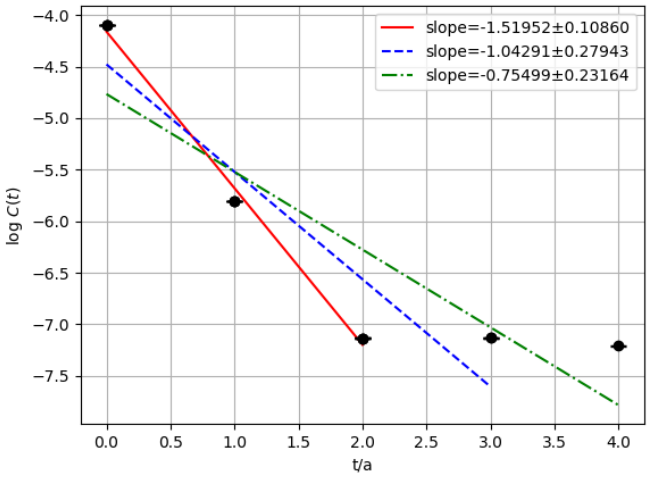

Figure C.2: The mass plot for the A_1^{++} glueball as determined from the 2x2 Wilson loop operator. Lattice size is $12^3 \times 18$, $\beta = 1.8$, with mulithit. The three lines correspond to determining the mass from the first 3, 4, and 5 data points. mass $= -$slope

Multihit 2x2 loop $\beta = 2.2$

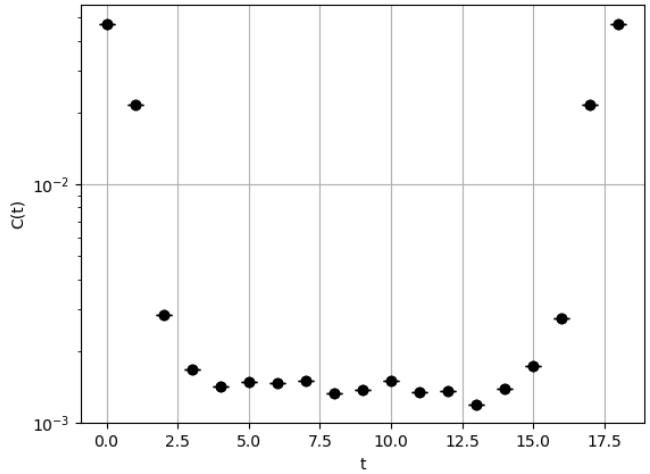

Figure C.3: The correlation for the 2x2 Wilson loop as a function of time, in SU(2) with lattice size 18×12^3, $\beta = 2.2$ with multihit applied

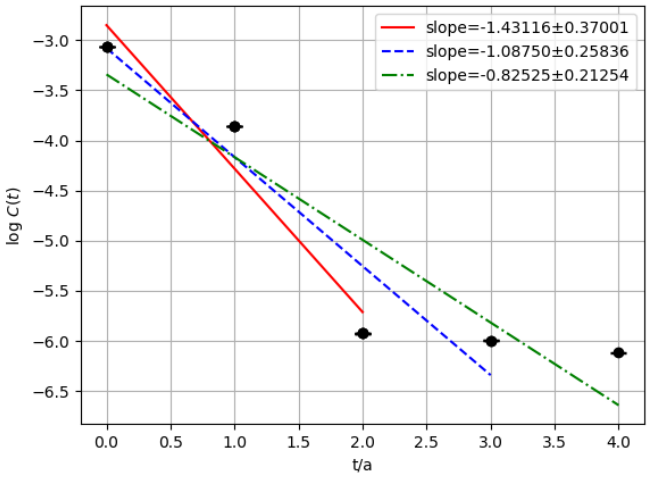

Figure C.4: The mass plot for the A_1^{++} glueball as determined from the 2x2 Wilson loop operator. Lattice size is $12^3 \times 18$, $\beta = 2.2$, with mulithit. The three lines correspond to determining the mass from the first 3, 4, and 5 data points. mass = −slope

Multihit + Multilevel 2x2 loop $\beta = 1.8$

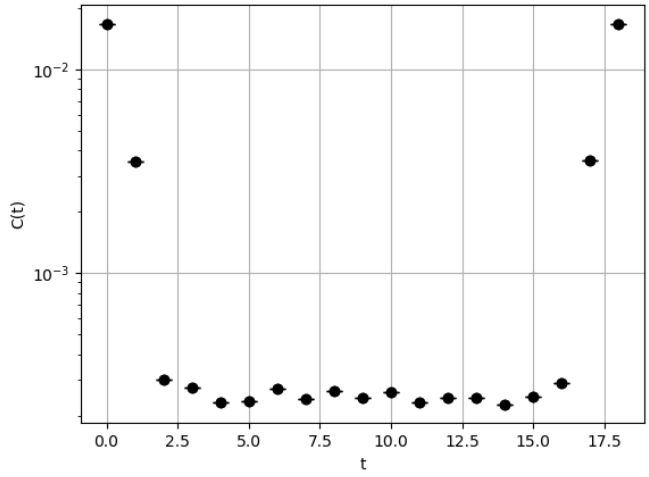

Figure C.5: The correlation for the 2x2 Wilson loop as a function of time, in SU(2) with lattice size 18×12^3, $\beta = 1.8$ with multihit and multilevel applied

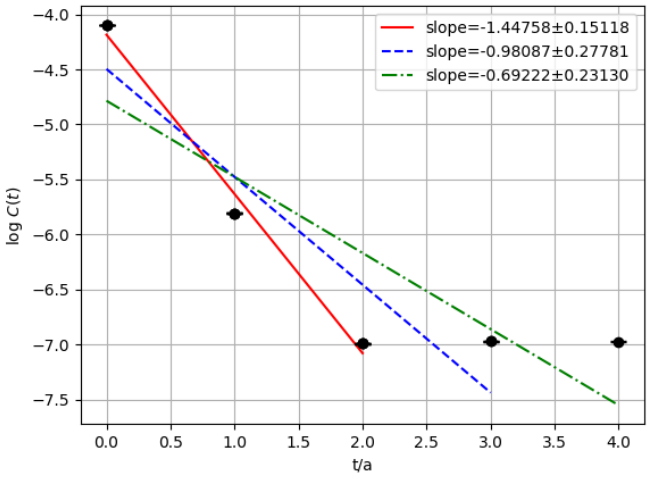

Figure C.6: The mass plot for the A_1^{++} glueball as determined from the 2x2 Wilson loop operator. Lattice size is $12^3 \times 18$, $\beta = 1.8$, with mulithit and multilevel. The three lines correspond to determining the mass from the first 3, 4, and 5 data points. mass $= -$slope

Multihit + Multilevel 2x2 loop $\beta = 2.2$

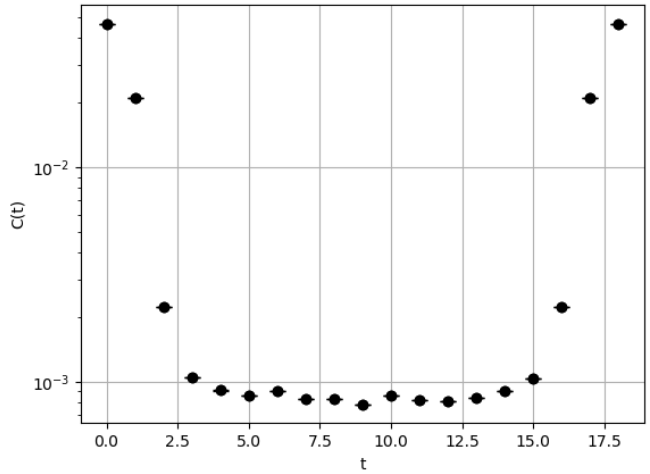

Figure C.7: The correlation for the 2x2 Wilson loop as a function of time, in SU(2) with lattice size 18×12^3, $\beta = 2.2$ with multihit and multilevel applied

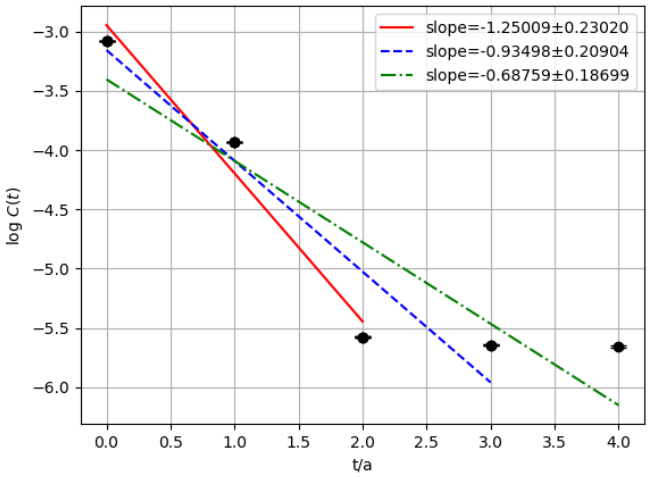

Figure C.8: The mass plot for the A_1^{++} glueball as determined from the 2x2 Wilson loop operator. Lattice size is $12^3 \times 18$, $\beta = 2.2$, with mulithit and multilevel. The three lines correspond to determining the mass from the first 3, 4, and 5 data points. mass = −slope

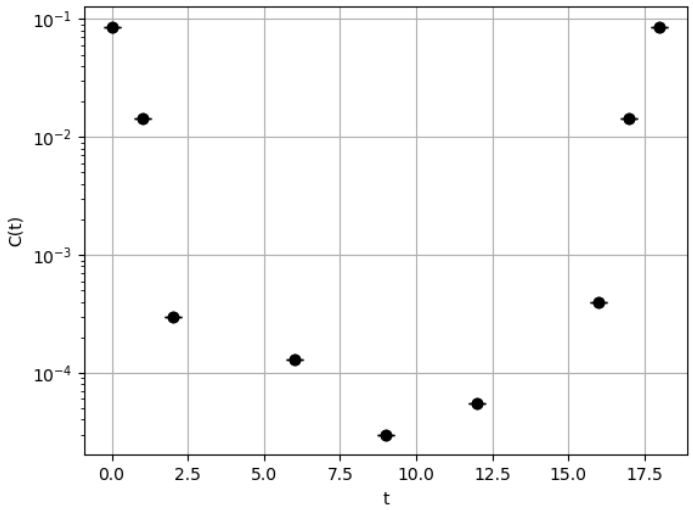

Figure C.9: The correlation for the E^{++} glueball as a function of time, measured by the double plaquette see B.2 and 4.6, in SU(2) with lattice size 18×12^3, $\beta = 2.0$, 20 measurements, with multihit and multilevel applied. Missing points are negative due to lack of statistics and not shown.